

N69- 16472  
NASA → CR-99280

Collisional Model of Asteroids  
And Their Debris

**CASE FILE**  
**COPY**

July 22, 1968

**Bellcomm, Inc.**

BELLCOMM. INC.

TR-68-710-4

Collisional Model of Asteroids  
And Their Debris

**CASE F**  
**COP**

July 22, 1968

J.S. Dohnanyi

Work performed for Manned Space Flight, National Aeronautics  
and Space Administration under Contract NASW-417.

TABLE OF CONTENTS

ABSTRACT	
I. INTRODUCTION . . . . .	1
II. OBSERVATIONAL EVIDENCE . . . . .	3
III. COLLISIONAL MODEL . . . . .	6
A. IMPACT MECHANICS . . . . .	6
B. COLLISION EQUATION . . . . .	12
IV. SOLUTION OF THE MODEL FOR ASTEROIDS . . . . .	24
V. APPLICATION AND DISCUSSION . . . . .	32
A. MODEL DISTRIBUTION . . . . .	32
B. STATISTICAL PROPERTIES OF ASTEROIDAL FRAGMENTS . . .	36
VI. CONCLUSION . . . . .	46
ACKNOWLEDGEMENTS	
VII. REFERENCES	
FIGURES 1 - 7	
DISTRIBUTION LIST	

ABSTRACT

A model for colliding objects in the asteroidal belt is formulated. An integro differential equation describing the evolution of a system of particles undergoing inelastic collisions and fragmentation is derived and solved for steady state conditions. It is found that the number density of particles per unit volume in the mass range  $m$  to  $m + dm$  is  $Am^{-\alpha}dm$  where  $A$  and  $\alpha$  are constants (provided that certain conditions are satisfied). The population index  $\alpha$  can then be derived theoretically; for asteroids and their debris,  $\alpha = 1.837$ , in agreement with an empirical fit to the observed distribution.

Various statistical properties of the distribution can be derived from the model. It is found that, for asteroidal objects, catastrophic collisions constitute the most important physical process determining particle lifetimes and the form of the particle distribution for particles sufficiently large that radiation effects are unimportant. The lifetime of the largest asteroids is found to be of the same order of magnitude as the probable lifetime of the solar system, therefore some of the largest asteroids may have survived since the time of creation; most smaller ones have not and are collisional fragments, according to the present model.

## I. INTRODUCTION

It is customary in the literature to describe the distribution of the masses of interplanetary particles by power law functions. The number of particles in a mass range  $m$  to  $m + dm$  is then taken to be  $A m^{-\alpha} dm$  where  $A$  and  $\alpha$  are constants; the latter is called the population index. Observational evidence in support of such a special form for the number density function has been advanced,\* among others, for radar meteors (Kaiser, 1961, Southworth, 1967), photographic meteors (Hawkins and Upton, 1958, Dohnanyi, 1966, 1967a) meteorites (Hawkins 1960) and asteroids (Kuiper et al, 1958). In an effort to understand the physical significance of population index type number density functions for interplanetary particles the writer has undertaken a theoretical treatment of the dynamic interaction of these particles. The physical model adopted is one where the interplanetary objects undergo mutual inelastic collisions resulting in fragmentation. Results of the analysis indicate that under plausible simplifying assumptions such a system of particles does indeed evolve into a population index type distribution (cf. Dohnanyi, 1967 b and c). The results are then applied to estimate the number density and other statistical properties of debris in the asteroidal belt.

Section II of this paper is a brief discussion of the empirical distribution of observed asteroids published by Kuiper et al (1958) together with a discussion of some of the statistical properties of power law distributions.

---

\*For a review of earlier work, see e.g., Lovell, 1954.

Section III-A of this paper is a discussion of the model crushing law when two objects inelastically collide. Experimental results by Gault et al (1965) and Gault and Heitowit (1963) are used for hypervelocity impact into semi-infinite targets; the results are then generalized for impacts between objects with similar masses.

Section III-B is the mathematical formulation of the model. An integro differential equation (which will be referred to as the collision equation) is derived, expressing the time rate of change of the number density of particles in a given mass range due to the processes of erosion, catastrophic collisions, and of particle creation in the same mass range by the collisional fragmentation of larger objects.

Section IV is a discussion of a mathematical model for which the collision equation is satisfied by a population index type solution. The result is that if the distribution has reached approximately steady state conditions, then a population index type solution does indeed satisfy the collision equation in a mass range sufficiently far removed from the high and low mass end points. The value of the population index is then calculated for various values of the average collisional velocity and found to be remarkably insensitive to the value of the physical parameters. The stability of the solution is also discussed.

The present results are applied in Section V to the distribution of asteroids and their debris. It is found that the theoretical value of the population index for a steady state distribution of particles moving with asteroidal velocities is within the margin of error of an empirical fit to the observed asteroids catalogued by Kuiper et al (1958). The theoretical number density function is then normalized to the observed asteroids; the resulting function forms the basis of

calculating various statistical properties of the distribution. Among these are particle creation and destruction rates, the mass loss due to radiation effects, particle life times and erosion rates.

## II. OBSERVATIONAL EVIDENCE

This section is a discussion of the distribution of known asteroids together with some of their statistical physical properties. In their survey of asteroids, Kuiper et al (1958) have published the distribution of 1554 asteroids as a function of absolute photographic magnitude  $g$  per half magnitude intervals.

The results of Kuiper et al (1958) are plotted in Fig. 1. The solid line histogram is the number of asteroids in each half magnitude interval as a function of  $g$ . A mass scale, based on a geometric albedo of  $.2 \times 3^{\pm 1}$  and material density of  $3.5 \times 10^3 \text{ kg/m}^3$  has been associated, by the writer, with the magnitude scale. The upper limit on the geometric albedo represents a completely white smooth surface and the lower limit corresponds to basalt. The nominal value of  $.2$  is the mean of the estimated geometric albedos of the asteroids Ceres, Pallas, Juno and Vesta\* (see, e.g. Sharonov 1964). The results is

---

\*This is a revision of the writer's earlier treatment (Dohnanyi, 1967) where asteroids were treated as Lambert reflectors with a spherical albedo of  $.1$ . While the uncertainties in the photometric properties of asteroids are considerable we believe this present treatment of asteroid masses is somewhat more realistic. The present results are, however, within the margins of uncertainty previously estimated by the writer.

$$\log_{10} m = 22.67 \mp .72 - .6g$$

where  $m$  is the mass of the asteroid (in Kg) having an absolute photographic magnitude  $g$  (i.e. relative photographic magnitude at a distance of 1 AU from both the earth and the sun).

The results of Kuiper et al are complete up to a limiting magnitude of  $g \leq 9.5$ , i.e., the observed number of these objects is believed to equal the true number. Above  $g \geq 9.5$ , the difference between the true and observed number of asteroids begins to increase due to selection effects. The dashed line histogram is the probable number of asteroids using the "completeness" factors of Kuiper et al (1958). These authors have tabulated the maximum and minimum probable numbers of asteroids and the dashed line histogram in Fig. 4 is their mean. We have plotted the estimated probable numbers up to the value where the correction factor, due to selection, is of the order of 2. When the correction factor is much greater than 2, considerable uncertainties may be present.

It can be seen from the figure that a straight line (on this double logarithmic plot) is a good representation of the data for asteroids with  $g$  greater than six. The solid straight line is a least squares fit, by the writer, with the result

$$f(m)dm \propto m^{-1.80 \pm .04} dm \quad (1)$$

where  $f(m)dm$  is the number of asteroids per unit volume of space in the small but arbitrary mass range from  $m$  to  $m + dm$  kilograms.

The number density function per unit mass eq. 1 has the general form

$$f(m) = \text{constant} \times m^{-\alpha} \quad (2)$$



There are a number of examples of power law type distributions, such as eq. 2, observed in nature. The observed distribution of meteoroids has generally the form eq. 2. Radio meteors have a population index  $\alpha = 2$  (McKinley, 1951, Weiss 1961, Elford, Hawkins and Southworth 1964, Southworth 1967) while Kaiser (1961) reported  $\alpha = 2.17$ . Visual and photographic meteors have been reported variously to have a population index  $\alpha = 2$  to 2.34 (see McKinley 1961 for a review; cf. also Dohnanyi 1966 and 1967a). Hawkins (1960) reported that the distribution of known meteorites has a population index of 2 for stones and 1.5 for irons.

We now tabulate, for future use, some of the properties of population index type distributions. Given that the largest mass present is  $M_\infty$  and  $\mu$  is the smallest and that  $(M_\infty/\mu) \rightarrow \infty$ , the results listed in Table-1 are readily obtained. The table lists expressions for the total mass  $M_T$ , the total number  $N_T$  and total cross sectional area  $\sigma_T$  of the system of spherical particles as a function of the population index  $\alpha$ . The normalization constant  $A$  can then be expressed in terms of the physical parameters  $M_T$ ,  $N_T$  or  $\sigma_T$  and the resulting expressions are listed in the columns labeled as  $A(M_T)$ ,  $A(N_T)$  and  $A(\sigma_T)$  respectively. The quantity  $\lambda$  is defined as

$$\lambda = (3\pi^{1/2}/4\rho)^{2/3}, \quad (3)$$

where  $\rho$  is the material density of the particles. It is readily seen that the cross sectional area of a sphere where radius  $r$  and mass  $m$  becomes

$$\pi r^2 = \lambda m^{2/3}. \quad (4)$$

It can be seen from Table 1 that the total mass of the system,  $M_T$ , does not depend on the small mass cutoff  $\mu$  for  $\alpha < 2$ . For such populations most of the mass of the system is contained in the largest objects  $M_\infty$ . When  $\alpha = 2$ ,  $M_T$  is a

logarithmic function of  $M_\infty$  and  $\mu$ . For  $\alpha > 2$ , essentially all the mass of the system is concentrated in the small particles  $\mu$ . Since a power law function varies faster than does a logarithmic function, we see that when  $\alpha = 2$ ,  $M_T$  is relatively insensitive to either  $\mu$  or  $M_\infty$  and is completely independent of  $M_\infty$  or  $\mu$  if their ratio  $M_\infty/\mu$  is kept constant. The total mass of the system is therefore seen to be distributed evenly over all particle sizes for  $\alpha = 2$ .

A glance at the column, in Table 1, headed by  $N_T$  reveals that for  $\alpha < 1$  most of the particles are large, for  $\alpha = 1$  there are many particles of all sizes and for  $\alpha > 1$  practically all the particles are small.  $\sigma_T$  behaves similarly inasmuch the whole effective collisional cross sectional area is concentrated into the largest objects for  $\alpha < 5/3$ ; for  $\alpha = 5/3$  the effective collisional cross sectional area is distributed over the entire size range and for  $\alpha > 5/3$  the entire cross sectional area is concentrated into the smallest objects of the population.

### III. COLLISIONAL MODEL

#### A. Impact Mechanics

Interplanetary space contains a very large number of objects having different masses and orbits and are believed to frequently collide with each other inelastically. When such a collision occurs at a sufficiently high relative velocity, fragmentation results. In the present study, the relative velocities will be comparable to those of particles in space traveling in different and sometimes intersecting orbits. The impact velocity will therefore be of the order of kilometers per second, which is sufficiently high to cause fragmentation.

TABLE 1

	$M_T$	$A(M_T)$	$N_T$	$A(N_T)$	$\sigma_T$	$A(\sigma_T)$
$\alpha < 1$	$A \frac{M_\infty^{2-\alpha}}{2-\alpha}$	$(2-\alpha) M_T M_\infty^{\alpha-2}$	$A \frac{M_\infty^{1-\alpha}}{1-\alpha}$	$(1-\alpha) N_T M_\infty^{\alpha-1}$	$A \ell \frac{M_\infty^{5/3-\alpha}}{5/3-\alpha}$	$\left(\frac{5}{3}-\alpha\right) \frac{\sigma_T}{\ell} M_\infty^{\alpha-5/3}$
$\alpha = 1$	"	"	$A \ell n \left( \frac{M_\infty}{\mu} \right)$	$\frac{N_T}{\ell n(M_\infty/\mu)}$	"	"
$1 < \alpha < \frac{5}{3}$	"	"	$A \frac{\mu^{1-\alpha}}{\alpha-1}$	$(\alpha-1) N_T \mu^{\alpha-1}$	"	"
$\alpha = \frac{5}{3}$	"	"	"	"	$A \ell \ell n \frac{M_\infty}{\mu}$	$\frac{\sigma_T}{\ell \ell n(M_\infty/\mu)}$
$\frac{5}{3} < \alpha < 2$	"	"	"	"	$A \ell \frac{\mu^{5/3-\alpha}}{\alpha-5/3}$	$\left(\alpha-\frac{5}{3}\right) \frac{\sigma_T}{\ell} \mu^{\alpha-5/3}$
$\alpha = 2$	$A \ell n \frac{M_\infty}{\mu}$	$\frac{M_T}{\ell n(M_\infty/\mu)}$	"	"	"	"
$\alpha > 2$	$A \frac{\mu^{2-\alpha}}{\alpha-2}$	$(\alpha-2) M_T \mu^{\alpha-2}$	"	"	"	"

Regarding the mass distribution of fragments produced during impact, the following type of crushing will be assumed:

$$g(m;M,M_2)dm = C(M,M_2)m^{-\eta} dm \quad (5)$$

Here,  $g(m;M,M_2)dm$  is the number of particles having a mass between  $m$  and  $m + dm$  produced during the impact of a mass  $M$  with another, larger mass  $M_2$ . The coefficient  $C(M,M_2)$  is a function of the colliding masses and  $\eta$  is a constant.

This particular crushing law eq. 5 is based on experiment (Gault, Shoemaker and Moore, 1963) and observation of impact into semi-infinite targets, corresponding to the case of  $M_2 \rightarrow \infty$  in eq. 5. The value of  $\eta$  reported is

$$\eta \simeq 1.8 \quad (6)$$

Use of a particular crushing law is one of the major assumptions in this paper. However, since evidence supports a crushing law of the general form of eq. 5 during hypervelocity impact, it will be adopted here to estimate the distribution of particles resulting from inelastic collisions at orbital velocities.

We shall now define  $C(M,M_2)$  in eq. 5 explicitly. Using Table 1 we obtain for the normalization constant of a number density function with a population index  $\eta < 2$ :

$$C(M,M_2) = (2-\eta)M_e M_b^{\eta-2} \quad (7)$$

where  $M_e$  is the total ejected mass, i.e., the total mass of the fragments produced during an impact between masses  $M$  and  $M_2$ ;  $M_b$  is the mass of the largest fragment produced.

When eq. 7 is substituted into eq. 5, the result is

$$g(m; M, M_2) dm = (2-\eta) M_b^{\eta-2} M_e m^{-\eta} dm . \quad (8)$$

We shall presently distinguish between two types of collisions. By erosive collisions we shall designate events when the target mass  $M_2$  remains intact after the collision except that it lost some small fraction of its mass. Catastrophic collisions constitute events when the target mass  $M_2$  (as well as the projectile) is completely shattered.

For erosive collisions we take

$$M_e = \Gamma M \ll M_2 \quad (9)$$

$$M_b = \Lambda M \ll M_2$$

where  $\Gamma$  and  $\Lambda$  are both functions of the impact velocity and material properties of the target as well as the projectile but not their masses.  $M_2$  is the mass impacted by  $M$  and the double inequality sign reflects the fact that the coefficients  $\Gamma$  and  $\Lambda$  refer to a semi-infinite target. It can be seen from eq. 9 that  $\Gamma$  is the total ejected mass per unit projectile mass and  $\Lambda$  is the mass of the largest fragment per unit projectile mass.

The use of eq. 9 is based on results from hypervelocity experiments discussed by Gault et al (1963). These authors find that the total ejected mass as well as the mass of the largest fragment during hypervelocity cratering into basalt is proportional to the projectile kinetic energy, and hence, to the projectile mass. These experiments were conducted at impact velocities over a range not exceeding 10 Km/sec and over a range of projectile kinetic energies from 10 joules to  $10^4$  joules approximately .

If

$$rM \approx M_2 \quad (10)$$

then eq. 8 breaks down because a hypervelocity impact into a relatively small target differs from the former (semi-infinite target) situation since the shock formed during impact will be reflected back toward the impact area rather than propagated away to infinity (i.e., dissipated). This is particularly significant for stones fracturing easily under tension. For these objects, a mass

$$M_2 \gg M \quad (11)$$

can still be completely shattered by the shock wave (generated during the event) which is reflected at the free surfaces and propagated inward as a tension wave.

In the absence of sufficient factual information describing this catastrophic process, the following will be assumed:

- (i) the largest mass  $M_2$  completely shattered by  $M$  is given by

$$M_2 = r'M \quad (12)$$

with  $M_e \equiv M + M_2$  and  $r' > r$ .

- (ii) when

$$M_2 > r'M$$

the semi-infinite target relations are valid and the collision is erosive.

Substituting these constants into eq. 7, one obtains an explicit expression for  $C(M, M_2)$  in terms of  $M$  for erosive collisions

$$C(M, M_2) \simeq C(M, \infty) = (2-\eta)\Gamma\Lambda^{n-2} M^{n-1}, \quad \Gamma'M \leq M_2 \quad (13)$$

For catastrophic impacts between two particles where  $\Gamma'M$  is greater than  $M_2$ , we take the total available mass  $M + M_2$  to be equal  $M_e$

$$M_e = M + M_2 \quad (14)$$

and obtain for catastrophic collisions

$$C(M, M_2) = (2-\eta)\Lambda^{n-2} (M + M_2)M^{n-2}, \quad \Gamma'M \geq M_2 \quad (15)$$

This relation, together with eq. 5 and 13 defines the model crushing law employed in this study.

Approximate numerical values for  $\Gamma$  and  $\Lambda$ , based on hypervelocity impact experiments into basalt by Gault et al (1963) are given in Table II at several impact velocities

TABLE II

V(Km/sec)	$\Gamma$	$\Lambda$
5	$1.3 \times 10^2$	$1.3 \times 10$
10	$5 \times 10^2$	$5 \times 10$
15	$1.1 \times 10^3$	$1.1 \times 10^2$
20	$2 \times 10^3$	$2 \times 10^2$

The value of  $r'$  is more difficult to estimate. Gault (private communication) observed that a basalt particle is completely shattered by a projectile  $10^{-3}$  times its mass, moving at 2 km/sec. Since  $r$  is about 20 at this velocity,

$$r' = 50 r \quad (16)$$

for this case. It will be assumed, in what follows, that this relation is valid for higher projectile velocities as well.

#### B. Collision Equation

In this section the mathematical formulation of the evolution of a system of inelastically colliding particles is developed. All objects will be assumed spherical and of identical material properties. Given that  $f(m,t)dm$  is the number of particles per unit volume having a mass between  $m$  and  $m + dm$  at a time  $t$ , this function will change as a result of collisions between the particles because many new ones are constantly created (by fragmentation) and others destroyed. The system itself possesses a "sink" in the sense that sufficiently small particles are removed by radiation effects.

In what follows, the system will be assumed sufficiently random that an effective average collisional velocity (independent of particle mass) is meaningful; the collision cross section is taken as the cross sectional area of the colliding spherical particles. This assumption is equivalent to the process of finding the motion of the center of mass of the system of particles, then switching to the center of mass coordinate system; the particle velocities will then be random, to a first approximation. Here we have invoked the analogy of a system of gas molecules in a moving box.

An equation defining the collective evolution of our system of particles can now be defined. The time rate of change of the number of particles in a mass range of  $m$  to



$m + dm$  is given, in a schematic form, by the following expression (individual terms are explained below):

$$\frac{\partial f(m,t)}{\partial t} dm = \begin{array}{l} \text{I} \\ \boxed{\text{rate of change of the number of particles}} \\ \boxed{\text{per unit volume and unit time in mass range}} \\ \boxed{m \text{ to } m + dm \text{ due to erosion of these parti-}} \\ \boxed{\text{cles by collisions with smaller ones.}} \end{array} + \begin{array}{l} \text{II} \\ - \boxed{\text{rate of loss, because of "catastrophic"}} \\ \boxed{\text{collisions, in the number of particles per}} \\ \boxed{\text{unit volume and unit time in the mass}} \\ \boxed{\text{range } m \text{ to } m + dm} \end{array} + \begin{array}{l} \text{III} \\ + \boxed{\text{number of particles in the mass range } m \text{ to}} \\ \boxed{m + dm, \text{ created per unit time and unit}} \\ \boxed{\text{volume by erosive and catastrophic colli-}} \\ \boxed{\text{sional crushing of larger objects}} \end{array} \quad (17)$$

Term I is the rate of change of the number of particles per unit volume and unit time in the mass range  $m$  to  $m + dm$  due to the fact that the masses are themselves changing in time. This is caused by collisional processes which erode particles into and out of the mass range  $m$  to  $m + dm$  with the passage of time. This expression is given by (Dohnanyi, 1967b)

$$\text{term (I)} = - \frac{\partial}{\partial m} \left[ f(m,t) \frac{dm}{dt} \right] d'm \quad (18)$$

where the prime on  $d'm$  is used to distinguish it from  $(dm/dt)dt$ .

Eq. 18 can be understood by noting that the bracketed expression  $f(m,t)(dm/dt)$  is a flux term in the sense that it equals the number of particles (per unit volume) per unit time whose masses change, because of erosion, past the fixed mass value  $m$ . If we consider a two dimensional "phase space" in the

two variables, mass  $m$  and time  $t$ , where all the particles in the sample are plotted as points moving along "trajectories"  $m_i = m_i(t)$  with  $i = 1, 2, \dots, N_T$  then the number of particles (per unit volume) moving past a fixed mass value  $m$  per unit time is  $f(m, t)(dm/dt)$ . The net rate of change in the number of particles in the fixed mass range  $m$  to  $m + d'm$  is then readily seen to be the "divergence" with respect to  $m$  of the flux  $f(m, t)(dm/dt)$  multiplied by the increment  $d'm$ . The negative sign in eq. 18 is necessary because if both  $f(m, t)$  and  $dm/dt$  increase (or both decrease) with increasing mass, more particles are lost from the mass range than are gained as can easily be verified.\*

We now estimate  $dm/dt$  which is the rate of mass loss of a particle with mass  $m$  undergoing erosive collisions with other masses that are not large enough to completely disrupt the particle with mass  $m$ .

The amount of mass removed in a single collision with a mass  $M$  is, according to eq. 9,

$$rM \quad (19)$$

The number of collisions that a mass  $m$  will experience (per unit time) with particles in a mass range  $M$  to  $M + dM$  is equal to the triple product of the geometrical cross sectional area of the (spherical) particles and the number density (per unit volume) of particles in the mass range  $M$  to  $M + dM$  and the mean collisional velocity:

$$K f(M, t) \left( M^{1/3} + m^{1/3} \right)^2 dM \quad (20)$$

$$\text{where} \quad K = \lambda \bar{V} \quad (21)$$

---

\* If, e.g.,  $f(m, t)$  decreases with mass, there will be more particles at a mass  $m$  than at  $m + d'm$ . If, further, the particle masses are decreasing faster at  $m$  than at  $m + d'm$  a net loss results.

Here  $\bar{V}$  is the average collisional velocity and  $\ell$  is defined by eq. 3.

The total mass removed from  $m$  per unit time due to all erosive collisions is then the product of eq. 19 by eq. 20 integrated over appropriate limits,

$$\frac{dm}{dt} = - \Gamma K \int_{\mu}^{m/\Gamma'} M f(M,t) \left( M^{1/3} + m^{1/3} \right)^2 dM \quad (22)$$

where  $\mu$  is the mass of the smallest objects present and  $m/\Gamma'$  is the smallest mass that completely disrupts  $m$  during a collision (cf. eq. 12).

Since  $\Gamma'$  is of the order of  $10^3$  or larger, the collisional cross sectional area can be taken to be

$$K \left( M^{1/3} + m^{1/3} \right)^2 \sim K m^{2/3} \quad (23)$$

Combining eqs. 18, 22 and 23 then yields

$$\text{term (I)} = \frac{\partial}{\partial m} \left[ \Gamma K m^{2/3} f(m,t) \int_{\mu}^{m/\Gamma'} M f(M,t) dM \right] dm \quad (24)$$

which is the number of particles gained, in the mass range  $m$  to  $m + dm$ , per unit volume of space and unit time because of erosive collisions.

We now substitute into eq. 24 a population index type number density function of the form

$$f(m,t) = A(t) m^{-\alpha} \quad (25)$$

and the following expression is obtained.

$$\text{term (I)} = - \frac{A^2(t) K \Gamma}{2-\alpha} m^{-\alpha} - 1/3 \left[ (2\alpha-8/3)(m/\Gamma')^{2-\alpha} (\alpha-2/3) \mu^{2-\alpha} \right] dm \quad (26)$$

where  $\alpha = 2$ .

Eq. 26 can be understood if we consider its value when

$$m \gg \Gamma' \mu \quad (27)$$

where  $\Gamma' \mu$  is the mass of the largest object completely disrupted when colliding with  $\mu$ . When  $\alpha > 2$ , the first term in the bracketed expression on the right hand side of eq. 26 can be disregarded (in comparison with the second term in brackets). When  $\alpha = 2$ , the result is a logarithmic expression. When  $\alpha < 2$ , the second term in brackets on the right hand side of eq'n 26 can be disregarded, with the result

$$\text{term (I)} = - 2(\alpha-4/3)(2-\alpha)^{-1} K A^2(t) \Gamma (\Gamma')^{\alpha-2} m^{-2\alpha+5/3} dm \quad (28)$$

It can be seen, from eq. 28, that when  $\alpha > 4/3$  the right hand side of the equation is negative and erosion decreases the number of particles in any given mass range. When  $\alpha < 4/3$ , the right hand side of eq. 28 is positive and have more larger particles and eroded into the mass range  $m$  to  $m + dm$  (per unit time) than are eroded out (of the mass range) into smaller mass values. For  $\alpha = 4/3$ , term (I) vanishes, in first order, and hence the population is stationary with respect to erosion, i.e., as many particles are eroded into as are eroded out of the mass range  $m$  to  $m + dm$  per unit volume and unit time.

This completes our derivation of term (I) in the collision equation.

Term II in the collision equation (eq. 17) which is the time rate of change because of catastrophic collisions in the number of particles (per unit time and unit volume) having a mass in the range  $m$  to  $m + dm$  can be readily derived. We note that the number of collisions a particle (having a mass  $m$ ) experiences with other particles is eq. 20 integrated over appropriate limits. The total number of such events experienced by masses in the range  $m$  to  $m + dm$  per unit volume (and unit time) is then the product of the latter expression by  $f(m,t)dm$ . Therefore

$$\text{term II} = -K f(m,t)dm \int_{m/\Gamma'}^{M_\infty} f(M,t) \left( m^{1/3} + M^{1/3} \right)^2 dM \quad (30)$$

where the minus sign is used to denote a particle removal process and where  $M_\infty$  is the mass of the largest object present. The range of values for  $M$ ,  $m/\Gamma' \leq M \leq M_\infty$ , is seen to include all mass values that would completely disrupt  $m$  during an inelastic collision (cf. eq. 12).

Substitution of a population index type solution eq. 25 into eq. 30 yields, for masses  $m \ll M_\infty$ :

$$\begin{aligned} \text{term II} = & + \left[ A \ell m^{-\alpha+2/3} dm \right]_1 \left[ AV (m/\Gamma')^{-\alpha+1}/(-\alpha+1) \right]_2 \\ & - \left[ AV m^{-\alpha} dm \right]_3 \left[ M_\infty^{-\alpha+5/3}/(-\alpha+5/3) \right]_4 \quad \alpha \neq 5/3 \quad (31) \end{aligned}$$

where only the leading terms have been retained and terms describing grazing collisions disregarded. For  $\alpha = 5/3$ , a logarithmic expression results.

The expression labeled (1) in eq. 31 is the total cross sectional area of all particles in the mass range  $m$  to  $m + dm$  (per unit volume of space). Expression (2) is the

cumulative flux per unit area and unit time of point particles\* having a mass  $m/\Gamma'$  or greater, provided that  $\alpha > 1$ . (3) is the flux of point particles (per unit area and unit time having a mass in the range  $m$  to  $m + dm$ . (4) is the cumulative cross sectional area (per unit volume of space) of all particles having a mass  $M_\infty$  or smaller, provided that  $\alpha < 5/3$ .

It can therefore be seen that the rate of change in the number of particles (per unit volume and unit time) in the mass range  $m$  to  $m + dm$  due to catastrophic collisions given by eq. 31 is the sum of two separate contributions. On the one hand, one has expression (1) x (2) which is the rate of catastrophic collisions of our "target" masses  $m$  due to the influx of point particles with masses  $m/\Gamma'$  or greater. On the other hand, we also have expression (3) x (4) which is the rate of influx of our masses  $m$  into randomly spaced target objects. It can readily be seen that when  $\alpha > 5/3$ , the contribution of (3) x (4) is negligible. This happens because, when  $\alpha > 5/3$ , small particles are so abundant that catastrophic break ups of objects having a mass  $m$  are mainly caused by collisions with smaller objects having a mass in the neighborhood of  $m/\Gamma'$ . When  $\alpha < 5/3$ , the converse is true; (1) x (2) becomes negligible and the frequency of catastrophic encounters that objects with a given mass experiences is determined by their collision probability with the largest objects in the population. When  $\alpha = 5/3$ , both of these contributions are significant.

---

\*By the expression "point particle" a particle is meant that has no size i.e., all of whose mass is concentrated into a mathematical point.

Term (III) of the collision equation (eq. 17) is the number of particles, in the mass range  $m$  to  $m + dm$ , created per unit time and unit volume by the erosive and catastrophic fragmentation of inelastically colliding larger objects. It can be expressed (Dohnanyi, 1967b) in the form

$$\begin{aligned} \text{term. III} = K m^{-\eta} dm \int_{m/\Lambda}^{M_{\infty}} dM \int_M^{M_{\infty}} dM_2 C(M, M_2) f(M, t) f(M_2, t) \\ \times \left( M^{1/3} + M_2^{1/3} \right)^2 \end{aligned} \quad (32)$$

This expression can be understood in the following manner:

$$C(M, M_2) m^{-\eta} dm \quad (33)$$

is the number of particles created into the mass range  $m$  to  $m + dm$  by one single erosive or catastrophic collision between an object with mass  $M$  and a larger object of mass  $M_2$  (cf. eq. 5 and 12). The quantity

$$K f(M, t) dM f(M_2, t) dM_2 \left( M^{1/3} + M_2^{1/3} \right)^2 \quad (34)$$

is the total number of collisions per unit time and unit volume of objects having masses in the range  $M$  to  $M + dM$  with objects having masses in the range  $M_2$  to  $M_2 + dM_2$ . The quantity

$$K m^{-\eta} dm C(M, M_2) f(M, t) dM f(M_2, t) dM_2 \left( M^{1/3} + M_2^{1/3} \right)^2 \quad (35)$$

is then the rate (per unit time and unit volume) of production of masses in the range  $m$  to  $m + dm$  by the collision of objects in the mass range  $M$  to  $M + dM$  with objects in the mass range  $M_2$  to  $M_2 + dM_2$  provided that the abundance of the latter is given by  $f(M,t)dM$  and  $f(M_2,t)dM_2$ , respectively.

Integrating eq. 35 over appropriate limits in order to estimate the contribution (to the particle creation in mass range  $m$  to  $m + dm$ ) of all permissible collisions between masses  $M$  and  $M_2$ , we obtain eq. 32.

Using eqs. 13 and 15,  $(C(M,M_2))$  can be expressed explicitly in eq. 32; the result is

$$\begin{aligned} \text{term (III)} &= K(2-\eta)m^{-\eta} \Lambda^{\eta-2} dm \\ &\times \left\{ \int_{m/\Lambda}^{M_\infty/\Gamma'} dM \int_M^{\Gamma'M} dM_2 (M+M_2) \left( M^{1/3} + M_2^{1/3} \right)^2 M^{\eta-2} f(M,t) f(M_2,t) \right. \\ &+ \Gamma \int_{m/\Lambda}^{M_\infty/\Gamma'} dM \int_{\Gamma'M}^{M_\infty} dM_2 \left( M^{1/3} + M_2^{1/3} \right)^2 M^{\eta-1} f(M,t) f(M_2,t) \\ &\left. + \int_{M_\infty/\Gamma'}^{M_\infty} dM \int_M^{M_\infty} dM_2 (M+M_2) \left( M^{1/3} + M_2^{1/3} \right)^2 M^{\eta-2} f(M,t) f(M_2,t) \right\} \end{aligned} \quad (36)$$

Here the first and third integrals refer to catastrophic collisions between masses  $M$  and  $M_2$  such that both are totally disrupted

$$\Gamma'M \geq M_2, \quad (37)$$



where  $\Gamma'M$  is the largest mass completely disrupted during a collision with  $M$ . The second integral refers to erosive collisions between masses  $M$  and  $M_2$  such that  $M_2$  behaves as an infinite target

$$\Gamma'M \leq M_2 \quad (38)$$

and the mass redistributed is just  $\Gamma M$ .

The third integral refers to catastrophic collisions between objects in the mass range  $M_\infty/\Gamma'$  to  $M_\infty$ . For test masses  $m$

$$m/\Lambda \geq M_\infty/\Gamma' \quad (39)$$

where  $m$  is the largest fragment created during impact by a "projectile" object of mass  $m/\Lambda$ , the first two integrals are zero and only the third integral is retained with lower limit of  $m/\Lambda$  replacing  $M_\infty/\Gamma'$ .

We now substitute a population index type number density function, eq. 25 into, eq. 36. The result is

$$\text{term III} = m^{-\eta} dm \left\langle C(m/\Lambda, \Gamma'm/\Lambda) \right\rangle \quad (40)$$

where

$$\left\langle C(m/\Lambda, \Gamma'm/\Lambda) \right\rangle = \frac{2-\eta(\Gamma')^{8/3-\alpha}}{8/3-\alpha} \frac{KA^2 \Lambda^{2\alpha-11/3}}{2\alpha-\eta-5/3} m^{-2\alpha+5/3+\eta}. \quad (41)$$

where only the leading term has been retained; eq. 40 is valid under the following restrictions

$$\begin{aligned}
 (i) \quad m &<< \Lambda M_{\infty}/\Gamma' \\
 (ii) \quad \alpha &> 5/3 \\
 (iii) \quad \alpha &> \frac{1}{2} (n+5/3)
 \end{aligned} \tag{42}$$

where  $\Lambda M_{\infty}/\Gamma'$  is the largest fragment when  $M_{\infty}$  is completely disrupted by an object having a mass  $M_{\infty}/\Gamma'$ .

We now discuss the physical meaning of eqs. 40 and 41. Eq. 40 is the leading term arising from the contribution of catastrophic collisions to eq. 36. The contribution of erosive collisions is of the order of  $\Gamma/\Gamma' = 50^{-1}$  times (smaller than) eq. 40 for populations satisfying eq. 42-ii.

The comminution law, for a single catastrophic event is (eqs. 5 and 15)

$$g(m, M, M_2) = \left[ (2-n) \Lambda^{n-2} M_2 M^{n-2} \right] m^{-n} dm, \text{ for } M << M_2 \tag{43}$$

The expectation value of eq. 43 for all permissible collisions (per unit time and unit volume) between projectiles having masses  $m/\Lambda$  or greater and target masses of  $\Gamma'm/\Lambda$  or greater\* is eq. 40; the quantity  $\langle C(m/\Lambda, \Gamma'm/\Lambda) \rangle$  is the expectation value of the bracketed quantity in eq. 43.

---

\* This condition insures that at least some of the fragments will have a mass in the range  $m$  to  $m + dm$ .

Writing out term III (eq. 40) explicitly, we obtain for the number of particles created per unit volume and unit time

$$\text{term III} = \frac{(2-\eta)(\Gamma')^{8/3-\alpha}}{8/3-\alpha} \frac{KA^2 \Lambda^{2\alpha-11/3}}{2\alpha-\eta-5/3} m^{-2\alpha+5/3} dm \quad (44)$$

where the comminution law population index cancels from the mass exponent. This happens because the most important contribution to the creation of objects in the mass range  $m$  to  $m + dm$  arises from collisions where the mass  $m$  represents the mass of the largest fragments produced and, for a given number of collisions, the number of largest fragments produced is proportional to the number of collisions and not to the way smaller fragments are distributed. Mass, of course, must be conserved and the presence of the index  $\eta$  in the coefficient on the right hand side of eq. 44 partially insures this requirement.

In order that the dominating contribution to the production of masses in the range  $m$  to  $m + dm$  should consist in the largest fragments, it is necessary that the population index  $\alpha$  be greater than a certain value (condition (iii), eq. 41), otherwise large masses are so abundant that masses smaller than  $M_b$  will significantly contribute to the production rate eq. 40, and the exponent  $\eta$  will no longer cancel. Specifically this happens when

$$\alpha < \frac{1}{2} (+5/3) \quad (45)$$

i.e., when condition (iii), eq. 42 is violated.

If

$$\alpha < 5/3$$

i.e., if condition (ii), eq. 42 is violated, then large masses are sufficiently abundant that the catastrophic and erosive crushing of the largest objects (with masses in neighborhood of  $M_\infty$ ) will dominate the particle production rate eq. 36.

The influence of the large mass cutoff on the distribution at  $M_\infty$  also modifies the particle production rate (as one would expect). This complication is, however, absent for objects with relatively small masses satisfying condition (i), eq. 42.

It is interesting to note that when  $\alpha = 11/6$ , the dependence on  $\eta$  of the expression in eq. 44 cancels. The production rate of masses in the range  $m$  to  $m + dm$  is in this case simply proportional to  $m^{-2} dm$ .

#### IV. SOLUTION OF THE MODEL FOR ASTEROIDS

In this section, the collision equation (eq. 17) is solved for a special case and the significance of the solution discussed.

Substitution of the explicit expressions eq. 26, 31 and 44 for the various terms in eq. 17 yields (after cancellations)

$$\begin{aligned}
 m^{-\alpha} \frac{dA(t)}{dt} = & - \frac{2\alpha-8/3}{2-\alpha} A^2(t) K \Gamma(\Gamma')^{\alpha-2} m^{-2\alpha+5/3} \\
 & - \frac{A^2(t) K (\Gamma')^{\alpha-1}}{\alpha-1} m^{-2\alpha+5/3} \\
 & + \frac{2-\eta}{(2\alpha-\eta-5/3)(8/3-\alpha)} A^2(t) K (\Gamma')^{-\alpha+8/3} \Lambda^{2\alpha-11/3} m^{-2\alpha+5/3}
 \end{aligned} \tag{46}$$

where  $m^{-\alpha}(dA(t)/dt)dm$  is the rate at which the number of objects (per unit volume) in the mass range  $m$  to  $m + dm$  is changing in time. Eq. 46 is valid under the following restrictions (cf. eq. 42).

$$5/3 < \alpha < 2$$

$$\frac{1}{2} (n+5/3) < \alpha \quad (47)$$

$$\Gamma' \mu \ll m \ll \Lambda M_{\infty} / \Gamma'$$

where  $\Gamma' \mu$  is the largest object that can be completely disrupted when a particle of mass  $\mu$  collides with it and  $\Lambda M_{\infty} / \Gamma'$  is the mass of the largest fragment when the largest object in the sample  $M_{\infty}$ , is catastrophically broken up by an object having a mass  $M_{\infty} / \Gamma'$ .

It can be seen, that for  $\alpha$  not in the neighborhood of  $\alpha = 2$  but less than 2, the erosion term (first term on the right hand side of eq. 46) is smaller than the catastrophic collision particle removal term (second term) by a factor of the order of  $\Gamma / \Gamma' = 1/50$  and is negligible in a first approximation. It is therefore evident that erosion plays only a minor role in "shaping" the distribution of our particles (cf. discussion accompanying eq. 40).

The time dependent equation (eq. 46) can only be solved for constant  $\alpha$  if

$$-\alpha = -2\alpha + 5/3, \text{ i.e., } \alpha = 5/3 \quad (48)$$

This result, however, violates the first condition in eq. 47 and therefore gives rise to a contradiction. More specifically, for  $\alpha \leq 5/3$ , the particle creation term (term III) becomes, approximately,

$$\text{term III} = \frac{2-\eta}{(8/3-\alpha)(\eta+5/3-2\alpha)} A^2 K(\Gamma')^{\alpha-\eta+1} \Lambda^{\eta-2} M_{\infty}^{\eta-2\alpha+5/3} m^{-} \quad (49)$$

where use has been made of the relation

$$\eta \approx 1.8 > 5/3$$

It can be shown that for  $\eta < 5/3$ , similar (but not identical) conclusions apply.

From eq.30 it can easily be shown that when  $\alpha = 5/3$ , term III, eq. 49 is of the order of  $M_{\infty}^{\eta-5/3} (\Gamma'/\Lambda)^{2-\eta} m^{-\eta+5/3}$  times greater than is term II. It therefore follows, from eq. 46, that when  $\alpha = 5/3$  the fragmentation of large objects will definitely alter the distribution of particles since large quantities of objects with a population index  $\eta$  are added to the population of smaller particles. Whence the largest objects in the distribution give rise to an evolution of the whole system of particles. Equation 46 is obviously not satisfied for  $\alpha = 5/3$  and  $m \ll \Lambda M_{\infty}/\Gamma'$ .

The only way eq. 46 can be satisfied with constant  $\alpha$  is then the steady state solution

$$\frac{dA}{dt} = 0 . \quad (50)$$

We therefore have

$$\frac{(\Gamma')^{\alpha-1}}{\alpha-1} = \frac{2-\eta}{(2\alpha-\eta-5/3)(8/3-\alpha)} (\Gamma')^{-\alpha} + 8/3 \Lambda^{2\alpha-11/3} \quad (51)$$

where the erosion term has been disregarded and the quantity  $K A^2 m^{-2\alpha+5/3}$  factored out.

Eq. 51 is solved for

$$\alpha = 11/6 \quad (52)$$

which is the first approximation to the steady state solution.

Eq. 52 indicates that as long as  $\Gamma' \gg \Gamma$ , such that the erosion term (term I) can be disregarded, the steady state solution  $\alpha = 11/6$  is insensitive to the physical parameters  $\Gamma$ ,  $\Gamma'$ ,  $\eta$  (provided that  $\eta < 2$ ), and  $\Lambda$ . Thus, had we assumed that the physical parameters  $\Gamma$ ,  $\Gamma'$  and  $\Lambda$  depend on some power of the velocity other than two (i.e., kinetic energy scaling) the same results would follow regarding the first order approximation of the steady state value of  $\alpha$ . It is therefore evident that the result  $\alpha = 11/6$  for a steady state population is rather insensitive to the precise details of the impact mechanics used.

Some of the properties of a population with  $\alpha = 11/6$  can be discussed if one computes the total mass crushed catastrophically  $\dot{M}_{12}$ , by "projectile" objects in a mass range  $m_1$  to  $m_2$  impacting much larger target masses:

$$\begin{aligned}
\dot{M}_{12} &= \int_{m_1}^{m_2} A M^{-\alpha} dM \int_M^{\Gamma' M} M_2 K M_2^{2/3} A M_2^{-\alpha} dM_2 \\
&= \frac{K A^2 (\Gamma')^{-\alpha+8/3}}{(-\alpha+8/3)(-2\alpha+11/3)} \left( m_2^{-2\alpha+11/3} - m_1^{-2\alpha+11/3} \right) \\
&\qquad\qquad\qquad \text{when } \alpha \neq 11/6 \qquad (53) \\
&= \frac{K A^2 (\Gamma')^{-\alpha+8/3}}{\alpha + 8/3} \ln(m_2/m_1) \qquad \text{when } \alpha = 11/6
\end{aligned}$$

It can be seen, from eq. 53, that when  $\alpha > 11/6$ , the dominating term is  $m_1^{-2\alpha+11/3}$  for sufficiently great range of projectile masses (i.e., for  $m_2 \gg m_1$ ) and hence, practically all the crushed mass is produced by small projectiles. When  $\alpha < 11/6$ , the converse is true and practically all crushed mass is produced by large projectiles. When  $\alpha = 11/6$ , then the rate of mass production by crushing is independent from the mass of the projectile and is only a function of the ratio of the mass  $m_2$  of the largest and  $m_1$  of the smallest projectiles in the range considered. Therefore, when  $\alpha \neq 11/6$ , the rate of mass production is sensitive to the "end points"  $\mu$  or  $M_\infty$  in the distribution (depending on whether  $\alpha$  is greater or less than  $11/6$ , respectively) while for  $\alpha = 11/6$  the mass production is constant for fixed logarithmic intervals of projectile masses  $M_2/M_1$  and is therefore only a weak function of the "end points" (a change by a factor of  $e^{10}$  in the mass of either end point would only change the total mass production rate by a factor of 10).



The result  $\alpha = 11/6$  is based on the simplified relation, eq. 51. A more correct treatment has to consider the small (but finite) influence of erosion (term I) as well as the numerous higher order terms when the collision equation (eq. 17) is evaluated for a population index type number density functional (eq. 25) under the restricting conditions eq. 50. This program has been carried out by the writer and numerical values of the various collisional processes as a function of the population index  $\alpha$  are given in Fig. 2 and Fig. 3. These figures are plots, in units of  $(K A^2 m^{-2\alpha+5/3})^{-1}$ , of the number of particles per unit mass unit volume and unit time removed (or created) by the individual collisional processes and their sum for two different average collisional velocities, as indicated. The population index of the crushed fragments during each collision,  $n$ , is taken to be the experimental value 1.8. The value of  $\alpha$  at which the curve representing the sum of all processes crosses the horizontal axis (i.e., the value of  $\alpha$  at which the individual process adds up to zero) is the solution for  $\alpha$  of eq. 17.

It can be seen, from Figs. 2 and 3, that the particle creation term is significant only for values of  $\alpha$  lower than about 1.92 while erosion dominates for higher values of  $\alpha$ . The individual processes and their sums exhibit remarkably similar trends; the values of  $\alpha$  at which steady state is reached is  $\alpha = 1.841$  in Fig. 2 and 1.835 in Fig. 3. It can also be seen from Fig. 2 and Fig. 3 that if erosion were completely absent, the value of  $\alpha$  at which steady state is reached would be shifted toward the slightly higher value of about 1.842 to 1.845. If, however, the catastrophic collision process were absent, the steady state distribution would have a somewhat "steeper" population index of about 1.92 to 1.93. It can therefore be seen that the steady state distribution is determined by the balance of the creation and catastrophic collision processes and erosion has only a minor effect on the steady state distribution.

In view of the fact that the material parameter  $\Gamma$  is by a factor of 400 greater in Fig. 3 than in Fig. 2, we conclude that the value of  $\alpha$  at which steady state is reached as well as the relative trends of the individual collisional processes are insensitive to the material parameters, as we have deduced earlier. The same holds for  $\eta$ , since a modest variation in  $\eta$  is found to produce no significant departures. This is indicated in Table III. This table is a list of the values of  $\alpha$  for which steady state conditions have been reached, i.e., for which eq. 27 is satisfied, for various values of the parameters  $\Gamma$  and  $\eta$ ; the average collisional velocity for each case is also indicated. The interpolation error in the numerical value of  $\alpha$  is about  $\pm .0005$ .

TABLE III

	$\eta=1.7$	$\eta=1.8$	$\eta=1.9$	
$\Gamma$	$\alpha$	$\alpha$	$\alpha$	$\bar{V}(\text{km/sec})$
5	1.843	1.841	1.839	1
20	1.841	1.839	1.838	2
125	1.838	1.837	1.836	5
500	1.836	1.836	1.835	10
1125	1.835	1.835	1.835	15
2000	1.835	1.835	1.834	20

It can be seen, from the table, that the value of  $\alpha$ , at which a steady state is reached is in the range of  $1.834 < \alpha < 1.841$ , depending on the material parameters which range over several orders of magnitude. Higher collisional velocities tend toward a slightly lower equilibrium value of  $\alpha$  than do lower velocities and a small but significant change in  $\eta$  produces an insignificant change in the equilibrium value of  $\alpha$ .

We now examine the stability of the solution eq. 52. for small masses when steady state conditions are not fully satisfied and we allow  $\alpha$  to be slightly different from the steady state value and therefore a function of time.

The normalization constant  $A$  will now be rewritten in terms of the total mass of the system,  $M_T$ , and the mass of the largest object,  $M_\infty$  (cf. Table 1). One obtains

$$\frac{d}{dt} \left[ A m^{-\alpha} \right] = \frac{d}{dt} \left[ (2-\alpha) M_T M_\infty^{\alpha-2} m^{-\alpha} \right] \quad (54)$$

And hence

$$\begin{aligned} & M_T M_\infty^{\alpha-2} m^{-\alpha} \left[ (2-\alpha) \ln (M_\infty/m) - 1 \right] \dot{\alpha} \, dm \\ &= \left\{ - \left| \text{term II} \right| + \left| \text{term III} \right| \right\} dm \end{aligned} \quad (55)$$

where  $M_T$  and  $M_\infty$  are assumed constant as a first approximation. Since  $\alpha < 2$ , the expression in the bracket is positive for masses  $m$  somewhat smaller than  $M_\infty$ . Whence, when creation (term III) exceeds removal (term II) of particles in a mass range  $m$  to  $m + dm$  then  $\alpha$  increases in time. This merely reflects the fact that since each process of catastrophic collision adds a whole spectrum of particles having masses equal to or smaller than the size of the largest fragment, smaller particles are "piled up" faster than are larger ones and hence  $\alpha$  increases with time if this process is not balanced by a particle removal mechanism. If the removal term (term II) exceeds the creation rate (term III), then  $\alpha$  decreases with time. This follows since small particles, being more numerous than larger ones, undergo correspondingly more catastrophic collisions and therefore they will deplete faster (if not replenished) than do the larger objects, hence  $\alpha$  decreased with time in this case. Similar conclusions follow if term I (erosion) is included in eq. 55.

It can furthermore be seen, from Figs. 2 and 3, that, for a value of  $\alpha$  which is smaller than necessary to produce steady state, the particle creation process (term III) dominates. Eq. 55 indicates that in this case  $\alpha$  will increase with time toward the steady state value. If  $\alpha$  is greater than the steady state value, the particle removal processes will dominate and hence, by eq. 55,  $\alpha$  will decrease in time toward its steady state value. The steady state distribution is therefore shown to be stable by this simplified analysis.

## V. APPLICATION AND DISCUSSION

### A. Model Distribution

In this section, a model distribution of debris in the asteroidal belt is defined and compared with observation. This is accomplished by a suitable choice of the physical parameters and the number density function is then normalized to the observed number of asteroids.

In order to estimate the mean collisional velocity for asteroidal particles, we note that the overwhelming majority of asteroidal orbits have a very low eccentricity with an average value of about .15 (see, for example, Watson, 1956). This means that the asteroidal velocities are reasonably well approximated by their transverse component

$$V \approx 30/\sqrt{R} \quad (56)$$

where  $V$  is in Km/sec and  $R$  is the distance from the sun in AU.

Under this approximation, the relative asteroidal velocities  $V_{rel}$  become functions of only  $R$  and the orbital inclination  $i$ . Written explicitly,

$$\begin{aligned}
 v_{rel} &= \sqrt{v_1^2 + v_2^2 - 2v_1v_2 \cos(i_1 - i_2)} \\
 &= 30\sqrt{\frac{2}{R}} \sqrt{1 - \cos(i_1 - i_2)} .
 \end{aligned}
 \tag{57}$$

where the algebraic sign of  $i$  depends on whether the object is ascending or descending in its orbit.

In order to estimate the expectation value of  $1 - \cos(i_1 - i_2)$ , we make use of results published by Watson (1956). This author has discussed the distribution of the inclination of about 1500 asteroids and plotted the results; graphically. Assuming that the nodes are randomly distributed a symmetric function in  $i$  can then easily be constructed for the relative number of asteroids ascending in an orbit of inclination  $i$  (or descending in an orbit with "inclination"  $-i$ ). This program has been carried out by the writer with the result that the root mean squared average velocity\* is given by

$$\sqrt{\langle v_{rel}^2 \rangle} \simeq 5 \text{ Km/sec}
 \tag{58}$$

with a root mean square derivation of about the same magnitude. A value of  $R \simeq 3\text{AU}$  has been employed. Since the asteroidal belt extends from about 2 AU to about 3.5 AU, we expect that the region at  $R = 3\text{AU}$  is sufficiently close to the center of the asteroidal belt to be representative.

---

\*  $\langle v_{rel} \rangle = 0$  since the expectation value of  $\sqrt{1 - \cos(i_1 - i_2)}$  with respect to a symmetric distribution in zero; this merely reflects the fact that  $\bar{v}_{rel}$  points North as often as it points South.

Assuming that the distribution in inclinations of the observed asteroids is representative of the smaller ones, we take 5 Km/sec as the mean collisional velocity\* for our model. The population index of the steady state distribution for this velocity is then given in Table III, for  $\eta = 1.8$ ,

$$\alpha = 1.837 \quad (59)$$

We now consider again the distribution of the known asteroids as given by Kuiper et al, 1958 (cf Fig. 1). Fig. 4 is a plot of the number of asteroids as a function of absolute photographic magnitude  $g$  published by these authors and therefore is identical to Fig. 1 in this respect.

The solid straight line is an empirical least squares fit by the writer as in Fig. 1 and the resulting number density as a function of mass has a population index.

$$\alpha = 1.80 \pm .04 \quad (60)$$

The dashed straight line is a least squares fit to the data with a population index 1.837, (eq. 59). It can be seen, from the figure, that this relation fits the data reasonably well. The value  $\alpha = 1.837$  is, in fact, within the standard deviation of the empirical fit, eq. 60. The number of asteroids  $N(m)dm$  in the mass range  $m$  to  $m + dm$  in the asteroidal belt is then given by

$$N(m)dm = 2.59 \times 10^{16} m^{-1.837} dm \times 4^{\pm 1} . \quad (61)$$

In order to estimate the number density of asteroids in the mass range  $m$  to  $+dm$  we need to estimate the volume to which they are confined.

---

\*It can be shown that the spread in the orbital eccentricities of asteroids contributes a smaller relative velocity which, is negligible in view of the uncertainties already present in  $V_{rel}$ .

Narin (1956) has treated the distribution of the latitudes of the positions of 1563 asteroids and obtained an empirical fit giving the number of asteroids as a function of latitude in  $2^\circ$  intervals averaged for the years 1954 through 1974. Using Narin's result it is easy to show that about 81% of the 1963 asteroids are confined to a latitude of  $10^\circ$  or smaller. We therefore assume that asteroidal bodies are effectively distributed into a volume of revolution generated by a line inclined by  $10^\circ$  to the ecliptic and bounded by spheres with radii\* of 3.5 AU from the outside and 2 AU from the inside. The resulting volume is then  $8.47 \times 10^{34}$  meter<sup>3</sup>.

Assuming no correlation between asteroidal masses and inclinations, we normalize 81% of the asteroids to the volume of  $8.476 \times 10^{34}$  meter<sup>3</sup>. The result

$$f(m)dm = 2.48 \times 10^{19} m^{-1.837} dm/\text{meter}^3 \quad (62)$$

where  $f(m)dm$  is the number density of asteroids in the asteroidal belt per meter<sup>3</sup> in the mass range of  $m$  to  $m + dm$  Kg.

For the parameter  $M_\infty$  we choose the mass corresponding to  $g = 4$ ,

$$M_\infty = 1.88 \times 10^{20} \text{ Kg.}$$

This choice is, however, an extremely conservative lower limit. The number density of observed asteroids in the neighborhood of  $g = 4$  is (in a statistical sense) an order of magnitude higher than is the theoretical value given by eq. 61. If one divided the three largest asteroids into a fractional

---

\*This choice for the radial extent of the asteroidal belt coincides (approximately) with the region into which the asteroids of Kuiper et al's survey are distributed.

number of objects in the range of magnitudes  $6 > g > g_{\infty}$  where  $g_{\infty}$  corresponds to a fictitious but statistically meaningful object, the corresponding value of  $M_{\infty}$  is considerably larger than  $1.88 \times 10^{20}$  Kg. We do not carry out this program but will refer to it again before closing this section.

#### B. Statistical Properties of Asteroidal Fragments

In this section, a number of statistical properties of the distribution of asteroids and their fragments will be derived using the present collisional model and their significance discussed.

Using eq. 62, one can calculate the rate at which particles are undergoing collisional processes described by the model. The result is Fig. 5 where these rates are plotted logarithmically as a function of mass in Kg. Rates are expressed per year and are multiplied by the effective volume of the asteroidal belt so that the result is the total number of objects undergoing the various processes in the asteroidal belt (rather than per unit volume) within a latitude of  $\pm 10^\circ$ . The population index is taken equal to 1.837, the mean collisional velocity is 5 Km/sec and  $\eta$  is 1.80.

$\psi(m)dm$  is the total number of objects created per year in the mass range  $m$  to  $m + dm$  Kg, and is given by eq. 36 evaluated with the use of eq. 62 and multiplied by the volume of the belt (and expressed in appropriate units). We plot  $\psi(m) = \psi(m)dm/dm$  rather than  $\psi(m)dm$  so that the yearly rate corresponding to a certain value of  $m$  has to be multiplied by a desired mass range  $dm$  in order to obtain the number of objects yearly created in that mass range. We find, for example, that for  $m = 10^8$  Kg,  $\psi \approx 10^{-6}/(\text{yr Kg})$ . This means that if we take a mass range of



$10^8$  to  $10^8 + 10^7$  Kg, the yearly creation rate, in this range, becomes  $10^7$  Kg  $\psi \sim 10$ /year and hence, 10 objects in this mass range are created every year (on the average) by collisional break up of larger objects. The departure from linearity of  $\psi(m)$  at  $m \sim 10^{15}$  Kg is caused by the fact that one is approaching  $M_\infty$ , the top mass of the distribution.

The quantity  $\phi(m)dm$  is the number of objects in the mass range  $m$  to  $m + dm$  destroyed by catastrophic collisions per year and is given eq. 30, multiplied by the total volume and expressed in appropriate units. The numerical values of  $\psi(m)$  and  $\phi(m)$  are almost equal and are plotted in Fig. 5 as a single curve for masses less than  $10^{15}$  Kg; this reflects the relative unimportance of the erosion process in the steady state distribution described by the present model.

The expression  $\dot{M}(m)$  is the total mass in Kg of objects having a mass of  $m$  Kg or smaller created yearly due to collisional fragmentation; it is given by

$$\dot{M}(m) = \int_{\mu}^m \psi(m')m' dm' \quad (63)$$

where  $\psi(m)dm$  is given by eq. 36. It can be seen, from Fig. 5 that the total asteroidal mass, crushed yearly, is about  $10^{12}$  Kg (with an uncertainty of about  $\pm 1$ ).

For  $m$  sufficiently small, eq. 63 gives an estimate of the mass removed yearly from the asteroidal belt by radiation forces. Since in this model we have arbitrarily chosen  $\mu$  as the smallest object created,  $\dot{M}(\mu) = 0$ . It is, however, to be expected that objects with a mass  $\Gamma'\mu$  or less will be strongly influenced by radiation forces since they are no longer large enough to experience collisional processes by much smaller particles, the latter being absent because they are blown away by radiation pressure. We therefore assume, somewhat arbitrarily, that an upper limit of the yearly

mass loss from the asteroidal belt due to radiation damping (Robertson, 1936) and radiation pressure is given by  $M(\Gamma'\mu)$  in Kg/yr. According to Fig. 5, this quantity is about  $7 \times 10^{10}$  Kg/yr. In view, however, of the fact that the distribution of such small particles is likely to be strongly influenced by collisions with cometary meteoroids a reliable figure for the yearly mass loss can only be given after the problem under discussion has been treated. Whipple (1967) estimated the yearly mass input required to maintain the zodiacal cloud. He found that the total mass input of particles having a mass of .1 Kg or less is 10 or 20 tons per second (or  $3$  to  $6 \times 10^{11}$  Kg/yr). The total asteroidal mass of particles having a mass of  $10^{-1}$  Kg or smaller, is, from Fig. 5, about  $3 \times 10^{11}$  Kg/yr (with an uncertainty of  $\times 16^{\pm 1}$ ). Asteroidal particles may therefore contribute, significantly, to the zodiacal cloud. In order for the asteroidal particles to be dispersed into small perihelion orbits ( $< 1$  AU, for example), they must be so small that radiation damping is significant or else the collision responsible for the creation of the particles must involve a very large momentum transfer. It is therefore necessary to treat the dynamical interaction of the population of asteroidal particles with that of the cometary particles before one can precisely estimate the influence of asteroidal debris on the zodiacal cloud.

We note that when  $M(\Gamma'\mu)$  is averaged over a period of  $10^9$  years, the result is  $7 \times 10^{19}$  Kg which is the same order of magnitude (but smaller) as the mass of one of the largest objects present. This mass removal rate therefore requires the presence of one parent object in addition to others already available in very early times and therefore does not involve arbitrary assumptions.

We now consider the total mass  $M_T$  of the asteroids and their debris within a latitude of  $10^\circ$ . Using Table-1, we obtain

$$M_T = A(2-\alpha)^{-1} M_\infty^{2-\alpha}$$

Choosing  $M_\infty = 1.88 \times 10^{20}$  corresponding to an absolute magnitude  $g = 4$ , we obtain for the total mass density of  $3.1 \times 10^{-15}$  Kg/meter<sup>3</sup> (i.e., 3.1 milligrams/kilometer<sup>3</sup>) or a total mass of  $2.6 \times 10^{20}$  Kg. This latter value is of the same order of magnitude as the mass of one of the three largest asteroids. Practically all the mass in the asteroidal belt is therefore concentrated in the largest asteroids.

Fig. 6 is a double logarithmic plot of the rate  $\dot{R}$  at which the radius of a spherical object changes with time due to erosion as a function of the mass in Kg of the object; the radius of an object having a mass  $m$  and a density of  $3.5 \times 10^3$  Kg/m<sup>3</sup> is also indicated. The mathematical expression for  $\dot{R}$  is readily derived from eqs. 22, 25 and 62; the result is

$$\dot{R} = \frac{KA\Gamma}{(2-\alpha)(3g\pi\rho)^{1/3}} \left( (m/\Gamma')^{2-\alpha} - \mu^{2-\alpha} \right) \quad (64)$$

in an arbitrary system of units.

The most obvious feature of eq. 64 (cf. Fig. 5) is that  $\dot{R}$  is not a constant but a function of the mass of the object undergoing erosion. We remind the reader that the process of erosion as defined in this paper is not due alone to collisions with small micron sized particles but also to collisions with all masses up to  $m/\Gamma'$  where  $m$  is the mass of the objects being eroded. Since in our model the population index  $\alpha$  is less than 2, the particle number density is such that

the total mass eroded away from a given object by collisions with microparticles is much less than is the mass eroded away by larger objects. We therefore have a situation where objects that are large in comparison with microparticles are sufficiently abundant to dominate the erosion process. The erosion rate of an object with a given mass  $m$  is then determined by the abundance of all objects with masses less than  $m/r'$  which is the mass required to produce catastrophic break up of  $m$  and hence the nonlinear dependence of  $\dot{R}$  on  $m$ .

It can be seen, from Fig. 6, that  $\dot{R}$  of a particle increases with increasing particle mass. For large asteroids having a mass of  $10^{18}$  Kg, the erosion rate is of the order of a meter/ $10^6$  Yr which is a Km in  $10^9$  years. There is no way to check the accuracy of this figure, but we note that the lunar highlands are saturated with craters of a size range of tens of Km and smaller. Assuming most of these craters to be of impact origin and that the highlands have an age of the order of billions of years (and the maria are much younger), we note that if the moon did not possess a gravitational field it would surely be "eroded" to a depth of several kilometers. If the lunar impact environment has been comparable to that of the large asteroids, our result in Fig. 5 appears to be reasonable. In view of the fact that the impact environment of the moon has probably been less severe than is the environment in the asteroidal belt, at least for a very long time in the past our result in Fig. 5 appears to be reasonable.

The values of  $\dot{R}$  for small masses in Fig. 5 are not realistic since attention was not given to the influence of erosion by cometary meteoroids and spallation due to cosmic rays. These processes have been estimated by Whipple (1967) to give rise to an erosion rate not exceeding about  $50 \text{ \AA/yr}$

for stones. This upper limit is indicated in Fig. 5 as a horizontal dashed line. While Whipple's estimate applied to objects with orbits intersecting the earth's orbit, his upper limit is still meaningful for particles in the asteroidal belt if the erosive effect of cometary meteoroids in the asteroidal belt is taken to be comparable to or lower than is the case near earth.

Fig. 7 is a double logarithmic plot of particle life-times in years as a function of particle masses in Kg, as given by the present model; shaded area is the range of the systematic error because of the albedo\*. The lifetime of an object with respect to catastrophic collisions  $\tau_{cc}$  is taken as the inverse of the probability per unit time that the object will experience a catastrophic collision and is given by (cf. discussion preceeding eq. 30)

$$\tau_{cc}(m) = \frac{1}{K \int_{m/\Gamma}^{M_{\infty}} AM^{-\alpha} (m^{1/3} + M^{1/3})^2 dM} \approx \frac{m^{\alpha-5/3}}{KA \Phi} \quad (65)$$

where  $\alpha > 5/3$  and where  $\Phi$  is the result of performing the indicated iteration:

$$\Phi = \frac{(\Gamma')^{\alpha-1}}{\alpha-1} + 2 \frac{(\Gamma')^{-4/3}}{\alpha-4/3} + \frac{\gamma^{\alpha-5/3}}{\alpha-5/3}$$

---

\*The reader should bear in mind that, as has been pointed out, the shaded areas represent the ranges of systematic error but not that of random error. This means that if there is reason to revise downward the nominal value of asteroidal albedos, then ALL of the life times (provided with shaded areas) will have to be moved downwards from their nominal values by the same factor in Fig. 7.

Terms of the order of  $M_{\infty}^{-\alpha+5/3}$  and smaller have been omitted.

It can be seen, from eq. 65, that  $\tau_{cc}(m)$  is the mean collision time for particles of mass  $m$  with particles of mass  $m/\Gamma'$  or greater. Eq. 65 is an upper limit since during a time  $\tau_{cc}$  the mass of the object will continuously erode into smaller values and hence will have a smaller lifetime with respect to catastrophic collisions because  $\tau_{cc}$  decreases with mass, as indicated by eq. 65. This reflects the fact that, in the present model, the number of particles that can cause a disruptive encounter (for a given object) increases faster with decreasing particle mass than is the corresponding decrease in the collision cross section.

The value of  $\tau_{cc}$  for the largest asteroids is of the order of  $10^9$  years (cf. Fig. 7). If the average geometrical albedo of .2 for the four largest asteroids is representative, then the nominal curve for  $\tau_{cc}$  is the correct value for the asteroidal life times. It can be seen, from Fig. 7, that the life time of the six largest asteroids with masses  $m \geq 10^{19}$  Kg is equal to or greater than  $4 \times 10^9$  yr and therefore may have survived since the time of their creation (presumably  $4 \times 10^3$  years ago). The other asteroids have life times  $\tau_{cc}$  shorter than the life time of the solar system and may therefore be collisional fragments.

The lifetime with respect to erosion is defined by eq. 22 when the latter is integrated to obtain the particle mass as a function of time. The result is

$$t_E = \frac{(\Gamma')^{1/6}}{\Gamma K A} \left[ (\sqrt{2} - 1)m^{1/6} + (\Gamma'\mu)^{1/6} \ln \frac{\sqrt{2} m^{1/6} - (\Gamma'\mu)^{1/6}}{m^{1/6} - (\Gamma'\mu)^{1/6}} \right] \quad (66)$$

where we have taken, somewhat arbitrarily, the time for an object to erode to one half of its initial radius to represent the erosion lifetime  $\tau_E$ . A population index  $\alpha = 11/6 = 1.8333$  has been used to facilitate integration. The logarithmic term is significant only for masses approaching the value  $r'\mu$  as can be seen from Fig. 7. The definition of  $\tau_E$  is seen therefore to be different from that of  $\tau_{cc}$  since the latter is the inverse probability of complete destruction and represents, therefore, an effective lifetime.

It can be seen, from eq. 66, that  $\tau_E$  becomes infinite as  $m$  approaches  $r'\mu$ . The time for a particle to lose all its mass is also infinite for the same reason. Physically this happens because erosion stops for particles with masses smaller than  $r'\mu$ ; all collisions for such small particles are catastrophic.

We also plot, in Fig. 7, the particle lifetimes with respect to the Poynting Robertson effect  $\tau_{PR}$  and the lower limit of the lifetime of small objects  $\tau_L$  due to the influence of cometary meteoroids and cosmic rays estimated by Whipple (1967).  $\tau_L$  is defined here similarly to  $\tau_E$ , namely  $\tau_L$  is the time for erosion of an object to one half its radius.  $\tau_{PR}$  is taken here as the time required for an object to traverse radially one half of the asteroidal belt, because of radiation damping. It can be seen, from the figure, that for particles greater than about  $10^{-5}$  Kg (or 1 mm in radius) the process of catastrophic collision dominates the lifetime of the particles. Smaller particles may be subject to erosion by cometary particles to an extent that this latter mechanism dominates.  $\tau_E$  and  $\tau_{PR}$  are seen to be insignificant for all particles of reasonable size by comparison with  $\tau_{cc}$ .

Since  $\tau_{PR} \gg \tau_{CC}$  over the entire range of particle masses, we see that our neglect of radiation damping in the collision equation eq. 17 is justified.

It can also be seen, from Fig. 7, that the lifetime of the largest objects is of the order of  $10^9$  yr. Some of the large objects may therefore have escaped catastrophic collisions in the past, but most others have not. For small objects, having a mass of the order of perhaps  $10^{-5}$  Kg or smaller, the influence of collisions with cometary meteoroids must be treated, before meaningful lifetimes for these particles can be estimated, and therefore the significance of the curves in Fig. 7 for small masses is doubtful.

We now consider some aspects of self-consistency of the present model. The present method is applicable to masses smaller than about  $10^{18}$  Kg which is the largest fragment created when one of the largest objects,  $M_{\infty}$  having a mass of about  $10^{20}$  Kg is completely disrupted. This criterion is, however, overly conservative because of the three asteroids present with masses of about  $10^{20}$  Kg (cf. with Fig. 4). The presence of these large asteroids causes the effective value of  $M_{\infty}$  (and consequently also  $AM_{\infty}/\Gamma'$ ) to increase beyond the value of  $10^{20}$  Kg.

We now return to Fig. 4 and consider the significance of the close agreement between the population index  $\alpha = 1.837$  of the steady state solution and that of the empirical fit,  $\alpha = 1.80 \pm .04$ . The following two possibilities may be noted:

- (1) There is agreement between the empirical and the theoretical population indices because the effective value of  $M_{\infty}/\Gamma'$  is greater than is assumed in the model.
- (2) Agreement between the theoretical and empirical population indices for large asteroids is fortuitous.



Possibility (1) is plausible since an effective  $M_{\infty}$  can be defined; using Table-1, one can write for the total mass  $M_T$ :

$$M_T = AM^{2-\alpha} (2-\alpha)^{-1} \quad (67)$$

using a value for  $M_T$  of  $5 \times 10^{20}$  Kg which is the approximate total value of the total mass of the fragments as well as the mass of the three largest asteroids, eq. 67 can be solved for  $M_{\infty}$ . The result is an effective value for  $M_{\infty}$  of  $10^{22}$  Kg, and for  $AM_{\infty}/T'$  of about  $5 \times 10^{19}$  Kg implying that all asteroids with masses smaller than  $5 \times 10^{19}$  Kg are in a steady state distribution. Physically this means that the influence of the three largest asteroids on the distribution of smaller objects may be approximated to be similar to the influence of a fractional number of much larger objects when averaged over a long period of time. While a detailed treatment of this problem requires a more extensive analysis, the order of magnitude argument presented here is sufficient to establish the validity of applying this collisional model to asteroids.

Possibility (2) implies that the large asteroids are not in a steady state distribution. Since, however, masses of the order of  $10^{15}$  Kg or less are already in a steady state condition (cf. with Fig. 5) because the rate of particle creation equals the rate of particle removal of these masses, use of the density function eq. 62 appears justified for those and smaller masses even if the statistical significance of the largest asteroids is disregarded.

VI. CONCLUSION

A collisional model of interplanetary particles is formulated and applied to the distribution of asteroids and their debris. An integro differential equation has been derived which describes the collective dynamical interaction of these particles caused by inelastic collisions and fragmentation.

The collision equation has been solved for the particle number density function  $f(m) dm$  for the special case when the distribution has reached steady state conditions. The result is

$$f(m)dm = Am^{-\alpha} dm . \quad (68)$$

The population index  $\alpha$  equals  $11/6$  in a first approximation; higher order terms contribute only slightly to  $\alpha$  (cf. Table III). The value of  $\alpha$  is remarkably insensitive to the values of the physical parameters;  $\alpha$  changes from 1.834 to 1.843 when the parameters  $\Gamma, \Gamma'$  and  $\Lambda$  change by a factor of 400.

It is shown in the text that this solution is stable in the sense that if  $\alpha$  in eq. 68 is altered, an imbalance between the particle creation and removal rates is introduced which will cause the population index to return to its previous steady state value. It is furthermore shown (cf. Fig. 2 and 3) that for steady state conditions without an external source, the erosion rates have only a minor influence on the population when compared with the rates of catastrophic collisions and particle creation by fragmentation.

The results are then applied to the distribution of asteroids and their debris. The theoretical number density function for asteroids is (eq. 62).

$$f(m)dm = 2.48 \times 10^{19} m^{-1.837} dm/\text{meter}^3 \quad (69)$$

where the normalization constant is based on observation and the population index 1.837 corresponds to steady state conditions with a root mean square collisional velocity of 5 Km/sec. A systematic error of about half an order of magnitude may be present because of incomplete knowledge of asteroidal albedos.

A least squares fit to the distribution of asteroids (Fig. 4) catalogued by Kuiper et al (1958) yields an empirical value for  $\alpha$  of  $1.80 \pm .04$ . The theoretical value of  $\alpha$  is therefore seen to be within the margin or error of the empirical one.

Since the largest masses are not replenished the distribution (Fig. 4) assumes a quasi steady state condition for asteroids less than a given mass only (cf. Fig. 5). The approximate value of this mass depends on our choice for  $M_{\infty}$ . The most conservative choice of  $M_{\infty}$  is  $1.88 \times 10^{20}$  Kg corresponding to absolute photographic magnitude  $g = 4$  in Fig. 4; this implies steady state conditions for masses less than  $10^{16}$  Kg. Since the largest three observed asteroids cluster, they can be redistributed artificially according to the theoretical distribution, eq. 62 while keeping the total mass invariant. Such a procedure approximates the physical influence of the three largest masses on the dynamics of the population of smaller objects. The results implies that all but the largest asteroids have reached steady state conditions.

Using eq. 69, a number of useful statistical properties of asteroids can be calculated. The yearly total of asteroidal mass crushed is about  $10^{12}$  Kg/yr (Fig. 5). The amount of mass lost yearly from the asteroidal belt is about  $6 \times 10^{10}$  Kg but this figure may not be reliable because the influence on the population of small particles by cometary meteoroids has not been considered.

The total mass of asteroids and their debris is about  $2 \times 10^{20}$  Kg, where the three heaviest objects, of this same order of magnitude have not been properly included. When the top masses are considered, the total mass is of the order of  $5 \times 10^{20}$  Kg; it therefore follows that almost all of the mass in the asteroidal belt is concentrated in the three heaviest objects.

The erosion rate of an object in the asteroidal belt (Fig. 6) is nonlinear. The rate of change in the effective radius of the largest objects is about a meter/ $10^6$  yr. This rate decreases for smaller objects and for masses of about  $10^6$  Kg the rate equals 50 A/yr which is the upper limit caused by erosion of stones due to cometary particles and cosmic rays obtained by Whipple (1967).

The particle life times with respect to catastrophic collisions  $\tau_{cc}$ , erosion  $\tau_E$  and radiation damping  $\tau_{PR}$  have been calculated (Fig. 7).  $\tau_{cc}$  is found to be shorter than  $\tau_E$  by one and a half orders of magnitude.  $\tau_{cc}$  is also very much shorter than  $\tau_{PR}$  for micron sized or larger particles. For the largest asteroids,  $\tau_{cc}$  is of the order of  $10^9$  yr; these asteroids may have survived relatively undamaged since the time of their creation.

BELLCOMM, INC.

ACKNOWLEDGEMENTS

The writer is in debt to F.L. Whipple for some important suggestions and to A.H. Marcus, B.G. Smith and G.T. Orrok for helpful discussions and comments on the proof.

Thanks are also due to C.A. Friend for some of the numerical computations.

## BELLCOMM. INC.

### VII References

Dohnanyi, J.S. Model Distribution of Photographic Meteors, Bellcomm TR-66-340-1, 1966

Dohnanyi, J.S., Mass Distribution of Meteors, Astrophys J. 149, 735-737, 1967a

Dohnanyi, J.S., Collisional Model of Meteoroids, Proc. International Symposium on the Zodiacal Light and the Interplanetary Medium Honolulu, Hawaii, 1967-b and Bellcomm TR-67-340-3, 1967c

Dohnanyi, J.S., Collisional Model of Asteroids and Their Debris, International Symposium on the Physics and Dynamics of Meteors Tatranska Lomnica, Czechoslovakia, 1967-d

Elford, W.G., G.S. Hawkins, R.B. Southworth. The Distribution of Sporadic Meteor Radiants, Harvard Radio Meteor Project Research Report No 9, 1964

Gault, D.E. and E.D. Heitowit, The Partition of Energy for Hypervelocity Impact Craters Formed in Rock, Sixth Symp. Hypervelocity Impact, vol II part 2, 419-457, 1963

Gault, D.E., E.M. Shoemaker and H.J. Moore, Spray Ejected from The Lunar Surface By Meteoroid Impact, NASA TND-1767, 1963

Hawkins, G.S. and E.K.L. Upton, The Influx Rate of Meteors in The Earth's Atmosphere, Astrophys J. 128, 727-735, 1958

Hawkins, G.S., Asteroidal Fragments, Astro. J. 65, 318-322, 1960

Kaiser, T.R., The Determination of the Incident Flux of Radio Meteors, Monthly Not. Roy. Astr. Soc. 123, 265-271, 1961

Kuiper, G.P., Y. Fujita, T. Gehrels, I. Groeneveld, J. Kent, G. Van Biesbroeck and C.J. Van Houten, Survey of Asteroids, Astrophys. J. Suppl. Ser 3 289-428, 1958

Lovell, A.C.B., Meteor Astronomy, Oxford University Press, 1954

McKinley, D.W.R., Meteor Science and Engineering, McGraw-Hill Book Co., Inc. 1961

McKinley, D.W.R., Variation of Meteor Echo Rates with Radar System Parameters, Canadian J. of Phys. 29, 403-426, 1951

Narin, F., Spatial Distribution and Motion of the Known Asteroids, J.Spacecraft, 3, 1438-1440, 1966

Robertson, H.P., Dynamical Effects of Radiation in the Solar System, Monthly Not Roy. Astronom. Soc. 97, 423-438, 1936-1937

**BELLCOMM. INC.**

Sharonov, V.V., The Nature of the Planets, Israel Program for Scientific Translation, Jerusalem, 1964

Southworth, R.B., Space Density of Meteors, International Symposium on the Zodiacal Light and the Interplanetary Medium, Honolulu, Hawaii, 1967

Watson, F.G. Between the Planets, Harvard University Press, Cambridge, Mass. 1956

Weiss, A.A., The Distribution of Meteor Masses for Sporadic Meteors and Three Showers, Australian J. Phys. 14, 102-119, 1961

Whipple, F.L., On Maintaining the Meteoritic Complex., Smithsonian Astrophys Observatory Special Rep 239, 2-45, 1967

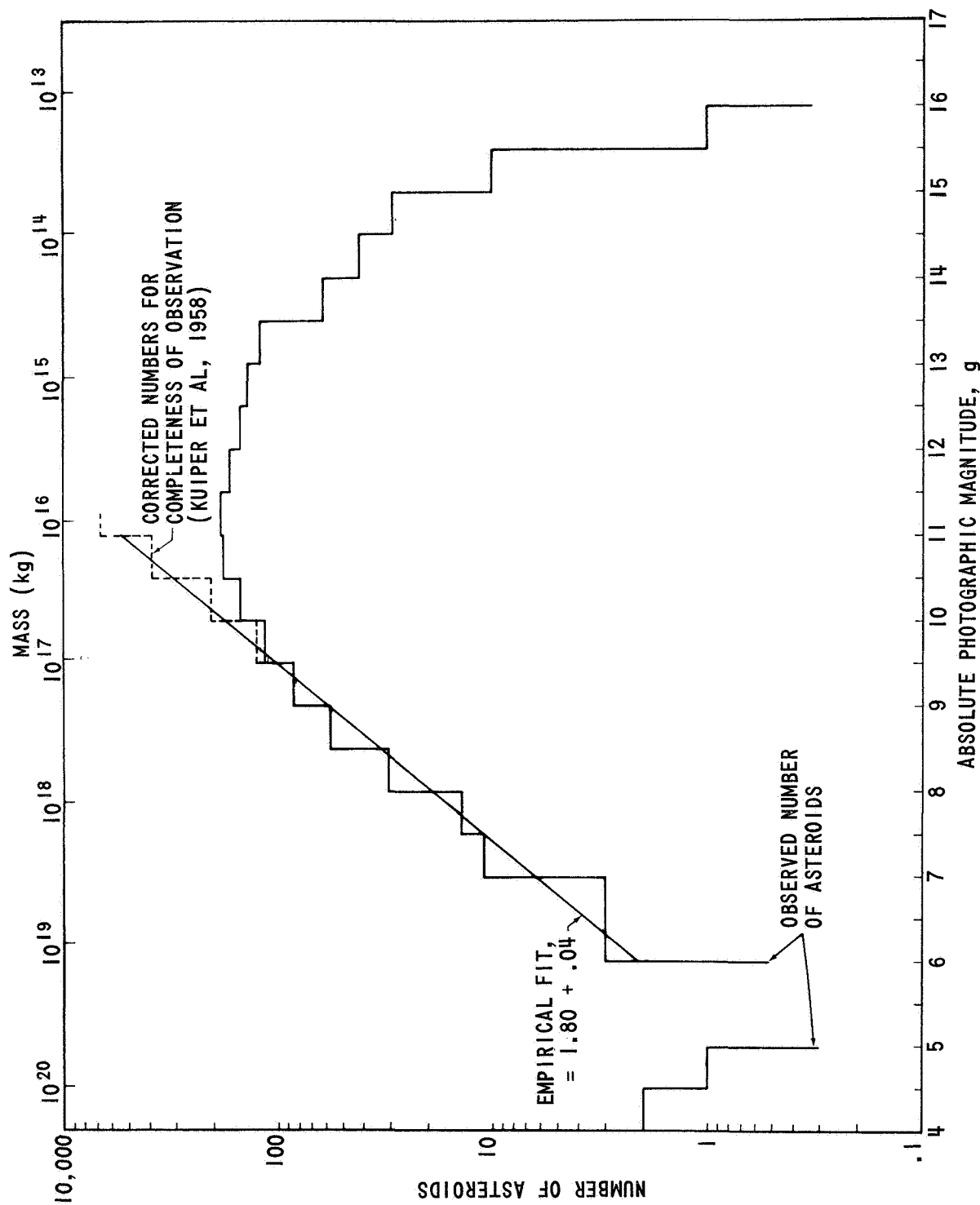


FIGURE 1 - TOTAL NUMBER OF OBSERVED ASTEROIDS (IN HALF MAGNITUDE INTERVALS) AS A FUNCTION OF ABSOLUTE PHOTOGRAPHIC MAGNITUDE (KUIPER ET AL, 1958). A MASS SCALE, ASSOCIATED WITH THE MAGNITUDE SCALE IS PLOTTED AT THE TOP OF THE FIGURE. DASHED HISTOGRAM IS THE PROBABLE NUMBER OF ASTEROIDS, BASED ON OBSERVATIONAL SELECTION. THE SOLID LINE IS A LEAST SQUARES FIT TO THE DATA (6 g 11) BY THE WRITER



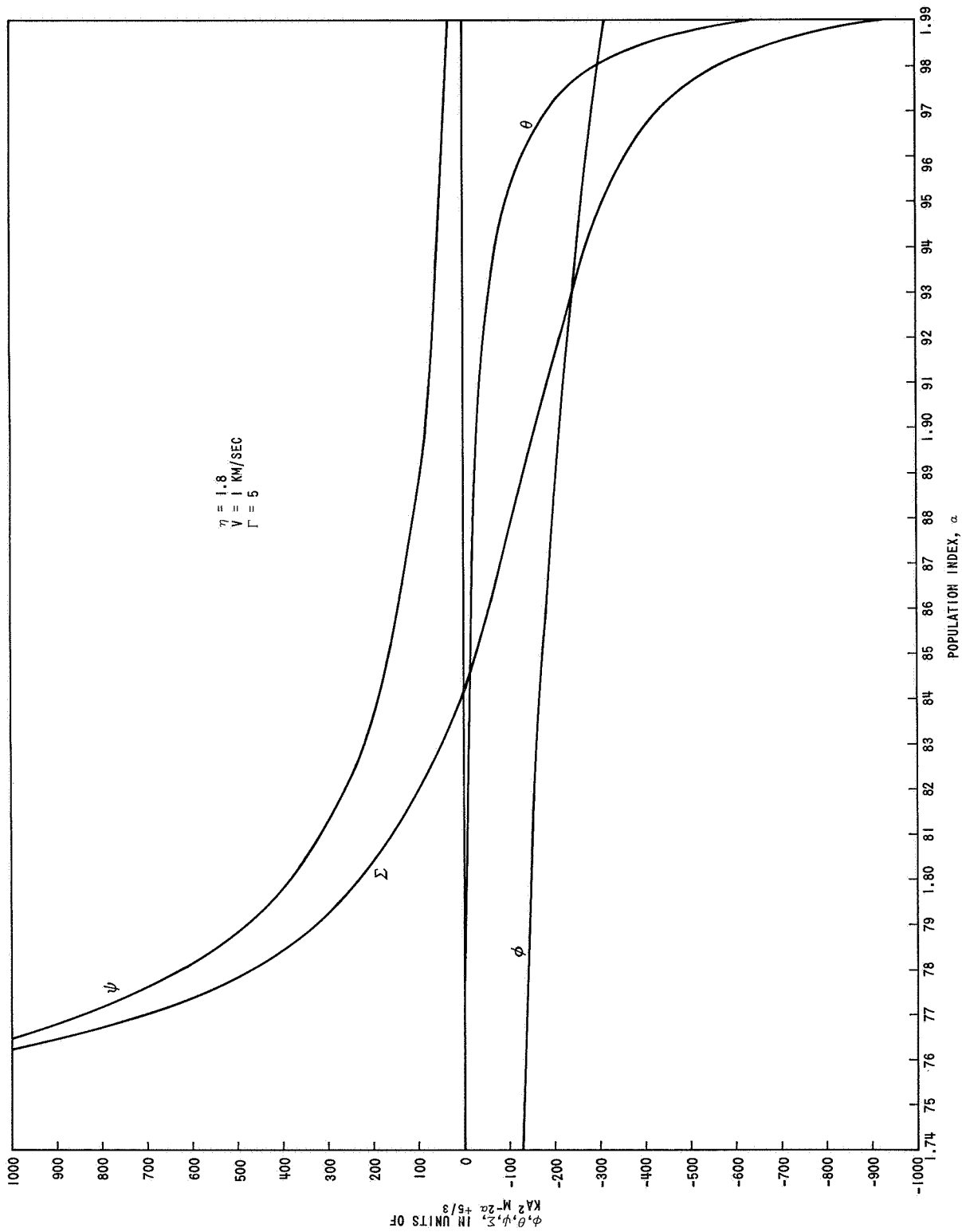


FIGURE 2 - RATE OF CHANGE OF THE NUMBER OF PARTICLES IN UNITS OF  $Ka^2 M^{-2a+5/3}$  PER UNIT TIME AND UNIT MASS RANGE AS A FUNCTION OF THE POPULATION INDEX  $\alpha$ .

$\psi$  = RATE OF CHANGE IN THE NUMBER OF PARTICLES BECAUSE OF PARTICLE CREATION BY FRAGMENTATION OF LARGER OBJECTS  
 $\phi$  = RATE OF CHANGE IN THE NUMBER OF PARTICLES BECAUSE OF CATASTROPHIC COLLISIONS  
 $\theta$  = RATE OF CHANGE IN THE NUMBER OF PARTICLES BECAUSE OF EROSION  
 $\Sigma = \theta + \phi + \psi$

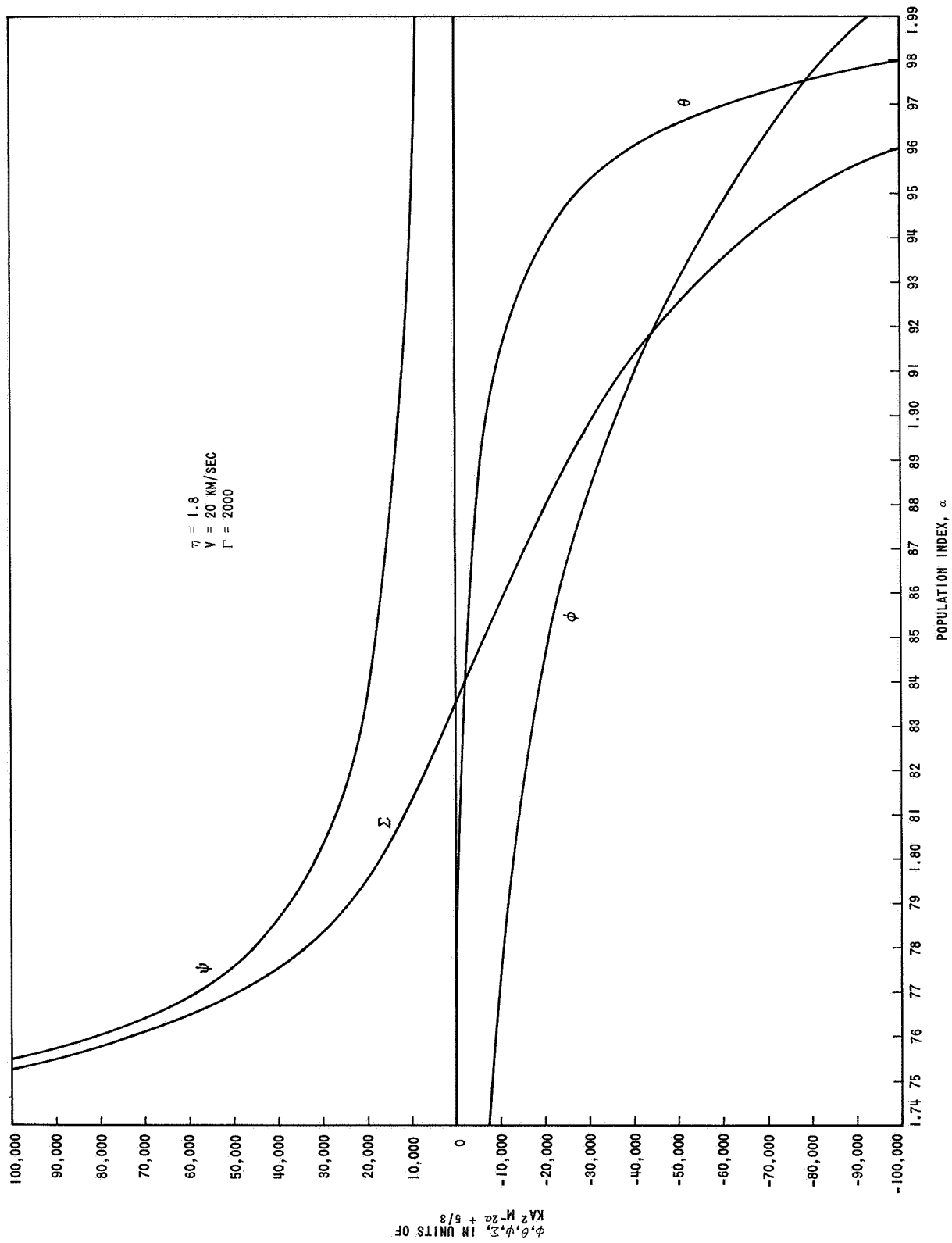


FIGURE 3 - RATE OF CHANGE OF THE NUMBER OF PARTICLES IN UNITS OF  $KA^2 M^{-2\alpha+5/3}$  PER UNIT TIME AND UNIT MASS RANGE AS A FUNCTION OF THE POPULATION INDEX  $\alpha$   
 $\psi$  = RATE OF CHANGE IN THE NUMBER OF PARTICLES BECAUSE OF PARTICLE CREATION BY FRAGMENTATION OF LARGER OBJECTS  
 $\phi$  = RATE OF CHANGE IN THE NUMBER OF PARTICLES BECAUSE OF CATASTROPHIC COLLISIONS  
 $\theta$  = RATE OF CHANGE IN THE NUMBER OF PARTICLES BECAUSE OF EROSION  
 $\Sigma = \psi + \phi + \theta$

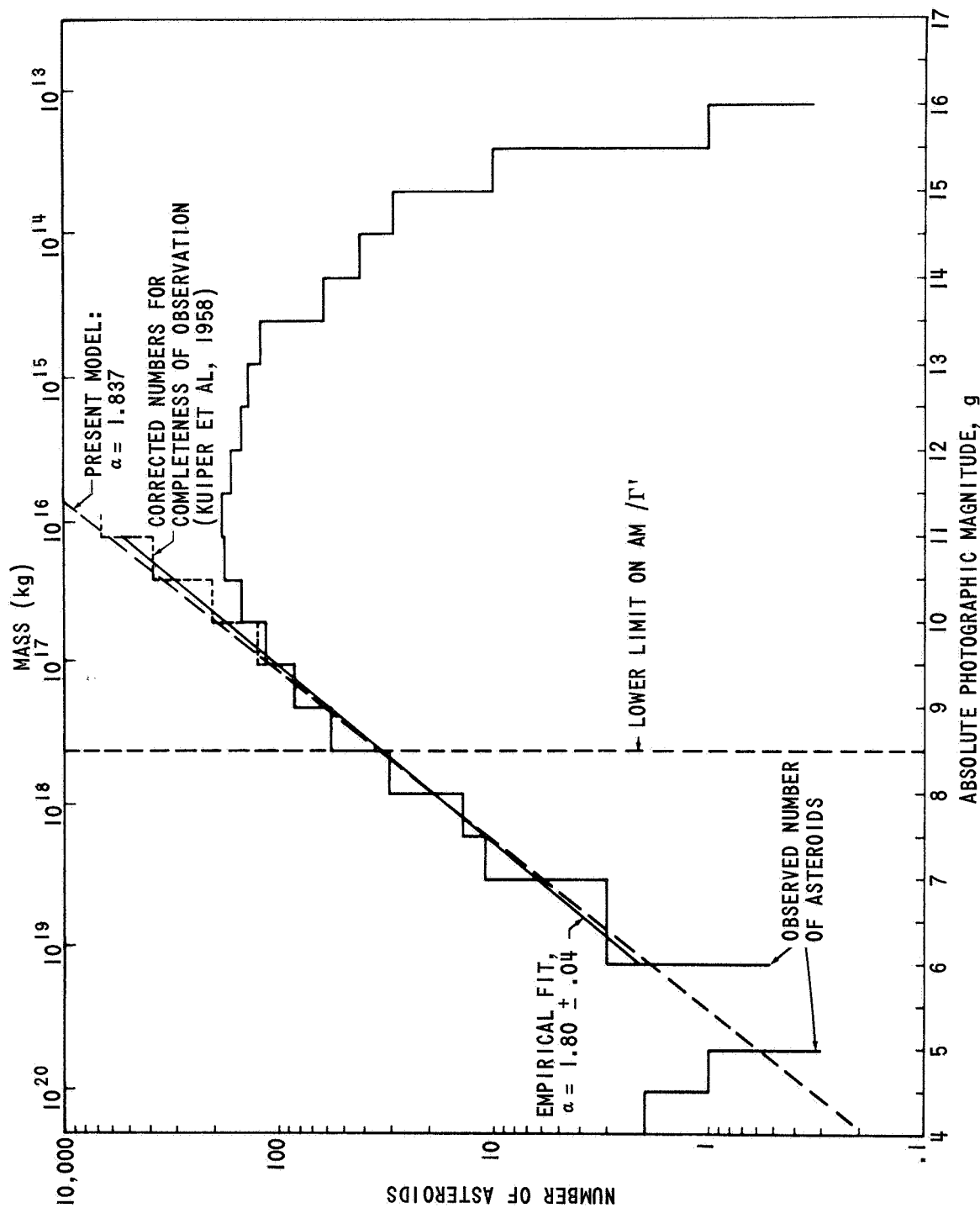


FIGURE 4 - TOTAL NUMBER OF OBSERVED ASTEROIDS (IN HALF MAGNITUDE INTERVALS) AS A FUNCTION OF ABSOLUTE PHOTOGRAPHIC MAGNITUDE (KUIPER ET AL, 1958). A MASS SCALE, ASSOCIATED WITH THE MAGNITUDE SCALE IS PLOTTED AT THE TOP OF THE FIGURE. DASHED HISTOGRAM IS THE PROBABLE NUMBER OF ASTEROIDS, BASED ON OBSERVATIONAL SELECTION. THE SOLID LINE IS A LEAST SQUARES FIT TO THE DATA (6 g 11) BY THE WRITER AND THE DASHED STRAIGHT LINE IS THE THEORETICAL RESULT DISCUSSED IN THE TEXT

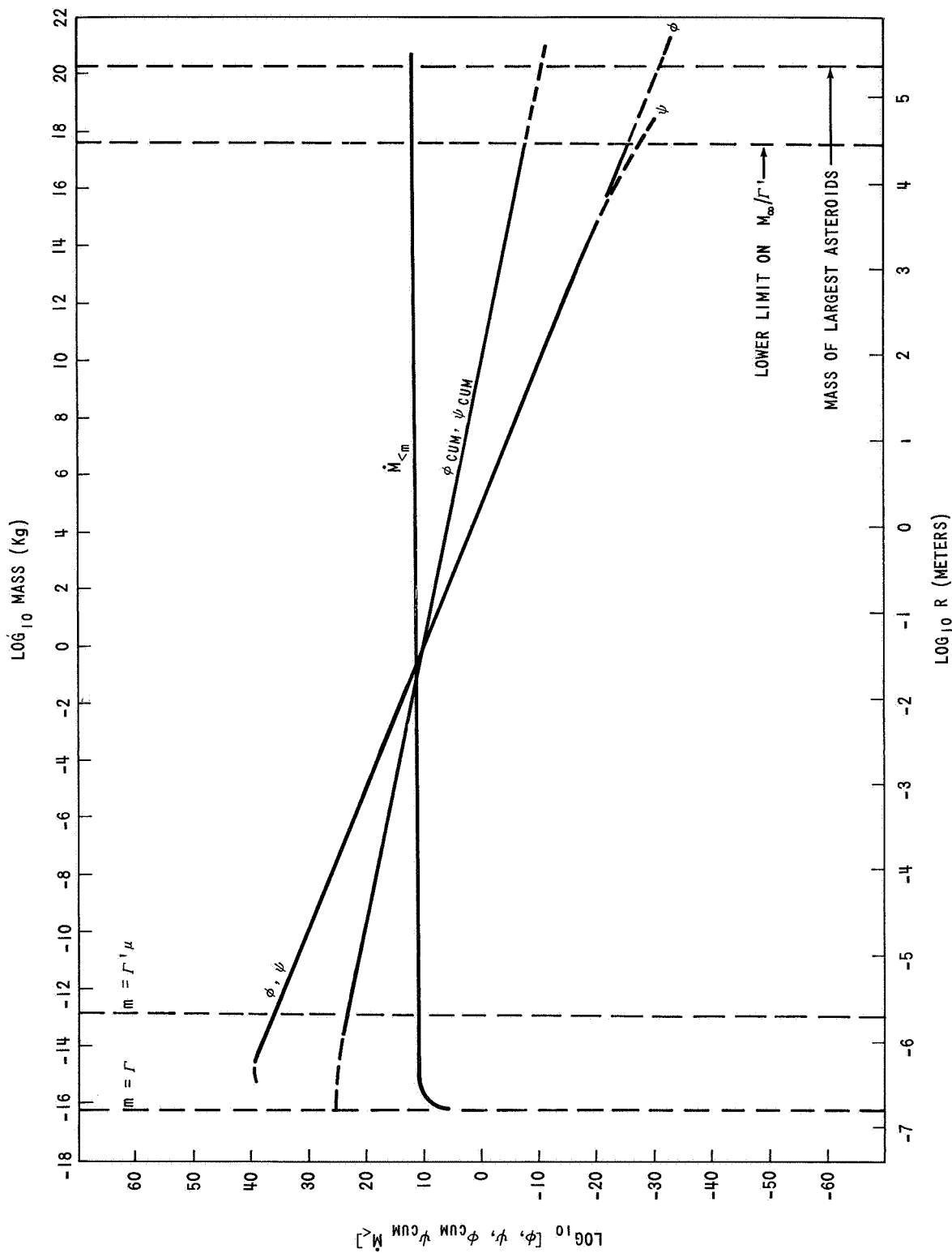


FIGURE 5 - THIS FIGURE IS A DOUBLE LOGARITHMIC PLOT AS A FUNCTION OF PARTICLE MASS (OR PARTICLE RADIUS) OF THE FOLLOWING YEARLY RATES:  
 $\phi, \psi$  PARTICLE REMOVAL RATE PER UNIT MASS DUE TO CATASTROPHIC COLLISIONS AND PARTICLE CREATION RATE PER UNIT MASS DUE TO FRAGMENTATION, RESPECTIVELY.  
 $\phi_{\text{cum}}, \psi_{\text{cum}}$ , SAME RATES CUMULATED OVER PARTICLE MASSES  $m$  OR LARGER.  
 $\dot{M}_{<m}$ , CUMULATIVE MASS OF PARTICLES WITH A MASS  $m$  OR SMALLER, CREATED ANNUALLY BY FRAGMENTATION

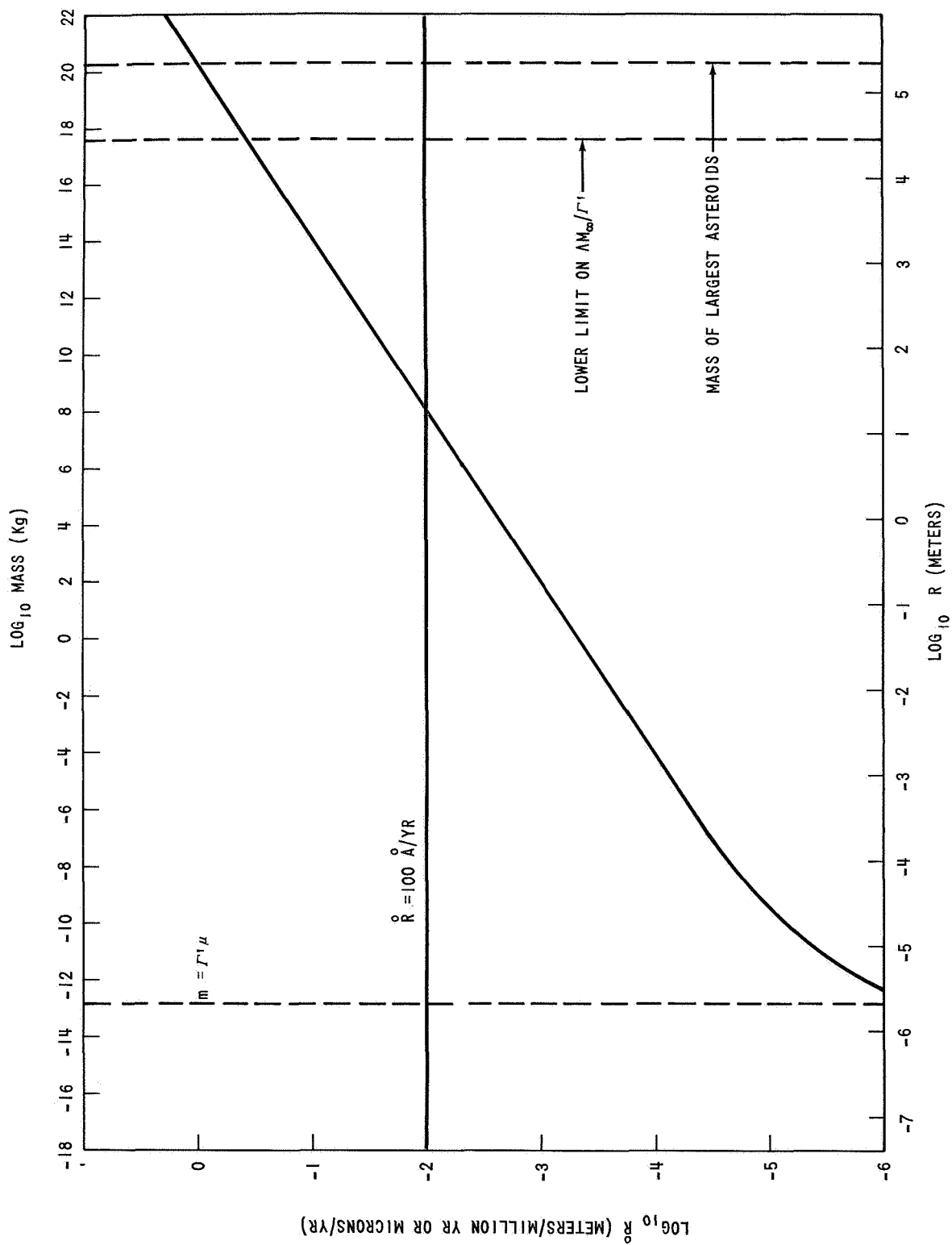


FIGURE 6 - STATISTICAL RATE OF CHANGE BECAUSE OF EROSION OF THE PARTICLE RADIUS IN METERS PER  $10^6$  YEARS (OR MICRONS PER YEAR) AS A FUNCTION OF PARTICLE MASS (OR PARTICLE RADIUS). THE DASHED HORIZONTAL LINE CORRESPONDS TO A LINEAR EROSION RATE OF  $50 \text{ } \mu/\text{yr}$ . SHADED AREA REFLECTS UNCERTAINTY IN THE ALBEDO

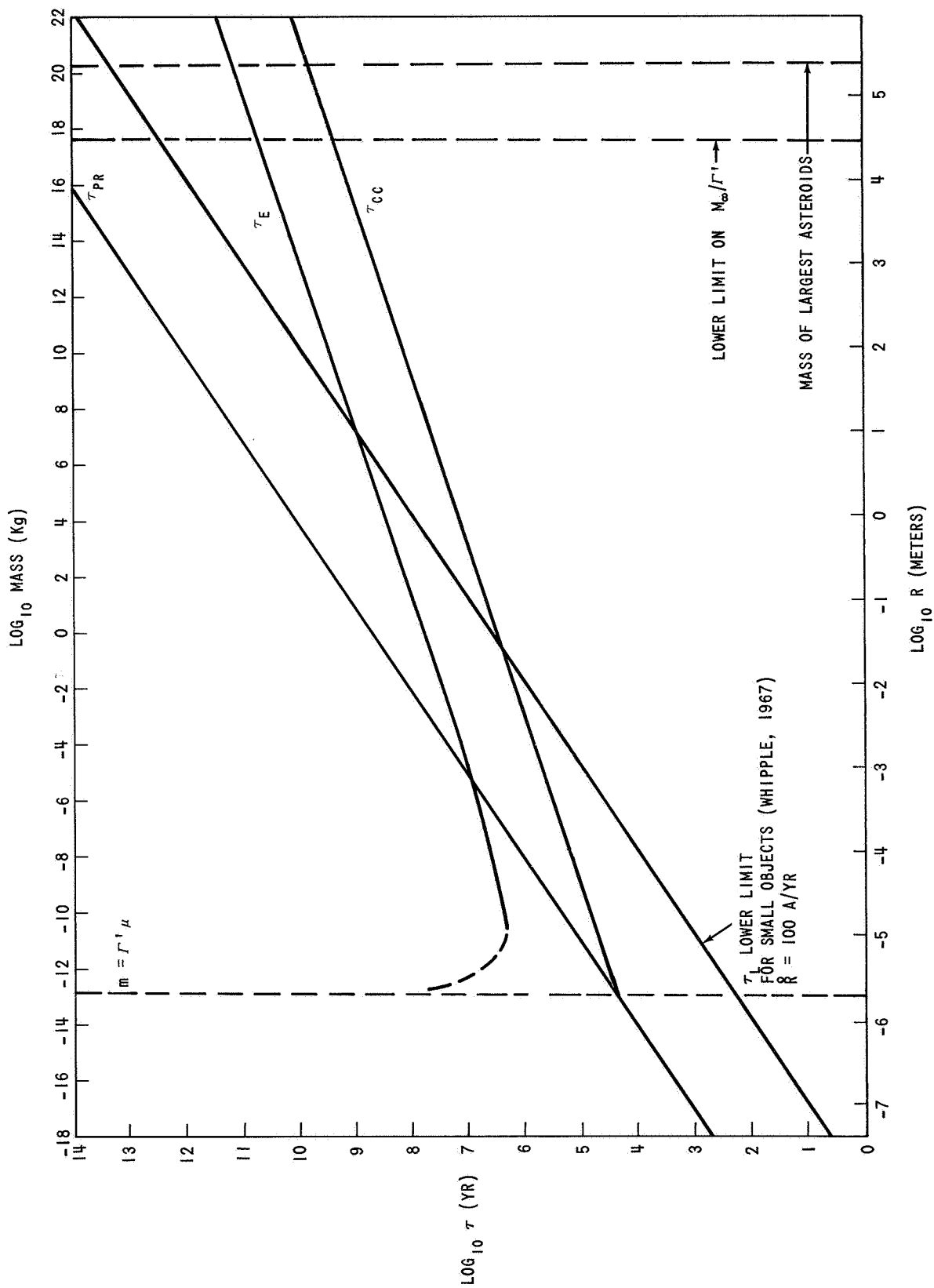


FIGURE 7 - DOUBLE LOGARITHMIC PLOT OF PARTICLE LIFE TIMES IN YEARS AS A FUNCTION OF PARTICLE MASSES IN KG (OR PARTICLE RADI IN METERS) SHADED AREA REPRESENTS UNCERTAINTY IN THE ALBEDO

# BELLCOMM, INC.

## DISTRIBUTION LIST

### NASA Headquarters

W.O. Armstrong - MTX  
W.C. Beckwith - MTP  
M.T. Charak - RV-1  
N.B. Cohen - RTP  
P.E. Culbertson - MLA  
C.T. D'Aiutolo - RV-1  
J.H. Disher - MLD  
F.P. Dixon - MTY  
M. Dubin - SG  
E.W. Hall - MTG  
T.A. Keegan - MA-2  
J.W. Keller - RV-1  
D.R. Lord - MTD  
S.C. Phillips - MA  
M.J. Raffensperger - MTE  
L. Reiffel - MA-6  
A.D. Schnyer - MTV  
J.H. Turnock - MT  
M.G. Waugh - MTP  
J.W. Wild - MTE  
NASA Hq. Library - USS-10 (2)

### NASA Manned Spacecraft Center

K. Baker - ET34  
P.B. Burbank - ET34  
B. Cour-Palais - ET34  
T. Giuli - TG5  
D. Kessler - ET34  
H.A. Zook - TG2

### NASA Marshall Space Flight Center

K.S. Clifton - R-SSL-PM  
C.C. Dalton - R-AERO-Y  
O.K. Hudson - R-RP-P  
W.G. Johnson - I/I/IB-P  
R.J. Naumann - R-RP-P  
R.E. Smith - R-AERO-YS

### NASA Langley Reserach Center

J.M. Alvarez - AMPD  
J.R. Davidson - 400  
D.D. Davis, Jr. - AMPD  
C.A. Gurtler - IRD  
W.H. Kinard - AMP  
C.H. Nelson - IRD

### NASA Goddard Space Flight Center

O.E. Berg - 613

### NASA Ames Research Center

H.J. Allen - D  
B.S. Baldwin - SST  
N.H. Farlow - SSP  
D.E. Gault - SSP  
C.R. Nysmith - SVHI  
L. Roberts - MAD (2)  
P.R. Swan - MS  
J.L. Summers - SVHI

### NASA Jet Propulsion Laboratory

A.S. Beck  
L.D. Jaffe

### NASA Lewis Research Center

I.J. Loefflet - 2732

### NASA Electronics Research Center

A.T. Lewis - CTR

### Aerospace Croporation

V.C. Frost

### Andrews Air Force Base

H.W. Brandly

### Baylor University

W.M. Alexander

### Bell Telephone Laboratory

A.A. Lundstrom

### Cornell University Center for Radio Physics and Space Research

M. Harwit

### Department of the Interior

S.F. Singer

### Douglas Aircraft

J.K. Wall

Dudley Observatory

C. Hemenway

General Motors Defense  
Research Labs

A.C. Charters

J.W. Gehring

I.T.T. Research Institute

F. Narin

Johns Hopkins University  
Department of Geology

M. Hallam

M.I.T. Lincoln Laboratory

I.I. Shapiro

Ohio State University  
Physics Department

J. Korringa

Rice University

J.J.W. Rogers

Smithsonian Astrophysical  
Observatory

G.S. Hawkins

R.E. McCrosky

W. Salisbury

R.B. Southworth

F.L. Whipple

TRW

J. Friichtenicht

University of California  
Institute of Geophysics  
and Planetary Physics

G.W. Wetherill

University of Chicago  
Enrico Fermi Institute for  
Nuclear Studies

E. Anders

University of Florida

A.E.S. Green

University of Hawaii  
Hawaii Institute of Geophysics

J.L. Weinberg

University of Maryland  
Dept. of Physics and Astronomy

L.W. Bandermaun

E.L. Opik

Bellcomm

F.G. Allen

G.M. Anderson

A.P. Boysen, Jr.

D.A. Chisholm

C.L. Davis

J.P. Downs

R.E. Gradle

D.R. Hagner

P.L. Havenstein

N.W. Hinnens

B.T. Howard

D.B. James

K.E. Martersteck

R.K. McFarland

J.Z. Menard

G.T. Orrok

T.L. Powers

I.M. Ross

F.N. Schmidt

C.M. Thomas

C.C. Tiffany

J.W. Timko

J.M. Tschirgi

R.L. Wagner

J.E. Waldo

All members Div. 101

Central File

Dept 1023

Library